ADAPTIVE CONTROL PERFORMANCE INDICATORS FOR INTERNAL COMBUSTION ENGINES

by

DAVID LAWRENCE NORTH

B.A.Sc., University of British Columbia
Vancouver, British Columbia, 1973

A THESIS SUBMITTED IN PARTIAL FULFILMENT OF

THE REQUIREMENTS FOR THE DEGREE OF

MASTER OF APPLIED SCIENCE

in the Department

of

Mechanical Engineering

We accept this thesis as conforming to the

required standard

THE UNIVERSITY OF BRITISH COLUMBIA

April, 1975

In presenting this thesis in partial fulfilment of the requirements for an advanced degree at the University of British Columbia, I agree that the Library shall make it freely available for reference and study. I further agree that permission for extensive copying of this thesis for scholarly purposes may be granted by the Head of my Department or by his representatives. It is understood that copying or publication of this thesis for financial gain shall not be allowed without my written permission.

Department of Mechanical Engineering

The University of British Columbia
Vancouver 8, Canada

Date April 2nd, 1975

ABSTRACT

The purpose of the investigation is to study the dynamics of the internal combustion engine-vehicle-driver system. Specifically, the system variables, engine angular velocity and engine angular acceleration are examined as potential observers of the engine mean torque. Such an observer is a requirement for the application of adaptive control to internal combustion engines. This type of control system has shown promise in providing solutions to the present problems of fuel economy, air pollution and performance.

A nonlinear dynamic model of the engine-vehicle-driver system is developed. This model is linearized and simplified to provide expressions for the variables of interest, the engine angular acceleration and velocity. The validity of the simplified model is established by comparison with results obtained from the computer simulation of the nonlinear model. The agreement between the two models is good.

The solutions of the equivalent system model are analyzed to determine which is the best observer for the mean torque. It is established that the steady state forced oscillatory engine angular acceleration response provides the best observer.

ACKNOWLEDGEMENT

I would like to thank Dr. T. N. Adams and Dr. R. E. McKechnie for their support and guidance throughout this work. The constructive criticism provided during the preparation of this thesis is particularly appreciated.

I would also like to thank my wife for her patience and understanding in typing the thesis.

TABLE OF CONTENTS

LIST OF TABLES

LIST OF ILLUSTRATIONS

NOTATION

Symbol	Description
Ap	vehicle projected area
$B\frac{1}{2}, B1, B\frac{3}{2}, \ldots$	Fourier sin torque series coefficients
$C\frac{1}{2}, C1, C\frac{3}{2}, \ldots$	Fourier cos torque series coefficients
Dc	equivalent linear clutch damping coefficients
Dt	tire damping coefficient
Dt'	equivalent tire damping coefficient at engine speed
Je	engine inertia
Jeq	equivalent system inertia
Jl	load inertia
Jl'	equivalent load inertia at engine speed
Kc	clutch spring constant
Kr	rolling resistance drag coefficient
Ks	driveshaft spring constant
Ks'	equivalent driveshaft spring constant at engine speed
Kt	tire spring constant
Kt'	equivalent tire spring constant at engine speed
Kl	ratio of the maximum to the mean torque per engine cycle
Nf	front wheel reaction

Symbol	Description
Nr	rear wheel reaction
R	rear end ratio
Rg	gear ratio
Rw	dynamic wheel radius
Tav	engine mean torque output
Tav#	optimum engine mean torque output
Tb	brake torque
Tc	nonlinear coulomb clutch damping
Te	engine instantaneous torque output
Tl	vehicle load torque
Tl'	equivalent vehicle load torque at engine speed
We	engine angular velocity
Wengi	initial engine velocity
Wn	natural frequency
Wnd	damped natural frequency
W	vehicle weight
|X|	magnitude of variable x
t	time
αeng	engine constant acceleration
θ	crank angle
θcx, $\dot{\theta}$cx, $\ddot{\theta}$cx	transient motions of variable x
θl	gradient angle
θs	spark timing
θsscx, $\dot{\theta}$sscx, $\ddot{\theta}$sscx	steady state constant motions of variable x

Symbol	Description
$\theta_{ssox}, \dot{\theta}_{ssox}, \ddot{\theta}_{ssox}$	steady state oscillatory motions of variable x
Γ	period of transient oscillation
Γ_c	transient time constant
ϕ_t	throttle position
τ	time of transient
ζ	damping ratio

1 INTRODUCTION

(1.1) Purpose and Scope

The chief problems of the current internal combustion automotive engine are air pollution, fuel economy and performance [1],[2],[3],[4],[5],[6],[7].[1] A concept which has shown promise in providing a solution to these problems is that of Adaptive Control [8],[9],[10]. Using this concept the present distributor advance unit and carburetor would be replaced by spark timing and air-fuel ratio devices regulated by an adaptive controller. The potential advantages of adaptive control include improved fuel economy, reduced emissions, reduced maintenance and improved reliability [8],[9],[10].

An adaptive control scheme requires a signal which indicates system output or performance. It has been shown by Adams [11] that for internal combustion engines the most suitable signal is the engine mean torque (T_{av}). The primary purpose of this work is to determine the best means of obtaining this torque signal. A secondary purpose is to construct a model of the dynamics of an engine-vehicle-driver system for later work in determining the optimum adaptive controller configuration.

---

[1] Numbers in square brackets designate references at end of thesis.

Any variable of the system which acts as an observer of T_{av} will be affected by disturbances acting on the system. Therefore, it is necessary to study the dynamics of the entire system to learn how a potential observer is affected by the disturbances encountered under normal operating conditions.

The dynamics of a lumped parameter engine vehicle system are considered in this work. An initial model is developed and its equations of motion are solved by simulation on the IBM 370 computer. This model is linearized and simplified to provide equations of motion which can be solved analytically. The validity of the linearization and simplification made is checked by comparison of the simulated and analytic solutions for a special case. The analytic solutions are used to evaluate potential observers for T_{av} .

In connection with this work, models describing the engine mean torque (T_{av}) and vehicle load torque (T_l) are developed. Some preliminary work on the adaptive control model and the human control model has also been undertaken. This work will be necessary in future to determine the optimum adaptive controller configuration.

(1.2) Work by Others

The recent work done in the application of automatic control theory to internal combustion engines falls into three categories, digital memory fuel injection control (DMC), closed

loop fuel injection control (CLC), and extremum seeking adaptive controls (AC).

(1.2.1) Digital Memory Fuel Injection Control

The DMC improves upon the conventional carburetor by eliminating the mechanical wear and aging problems [12],[13]. The memory stores predetermined optimum fuel injection pulse times. These pulse times are addressed by information derived from engine speed and throttle position. The drawback of this system is the predetermined nature of the stored information. For example, pulse times stored in the memory are obtained from tests on a standard engine under standard environmental conditions. These pulse times are optimum for this engine at the particular time they are determined.

However, production tolerances in engine manufacturing are not tight enough to assure that the pulse times will be optimum for every engine rolling off the assembly line. An even more serious problem is the wide range in environmental conditions a production engine will experience during its life. This range of environmental conditions definitely affects the optimum pulse time [14].

(1.2.2) Closed Loop Fuel Injection Control

The CLC senses the oxygen content of the exhaust gas stream and compares it with a reference value [14],[15]. If the measured value differs from the reference value, the control adjusts the fuel injection pulse time until the difference

disappears. This type of control was initially developed to insure satisfactory operation of catalytic converters by regulating the exhaust gas stream composition [14]. Later investigators [15] have extended the work to providing optimum air-fuel ratios, but the workers have not shown how this optimum may be identified.

(1.2.3) Extremum-Seeking Adaptive Control

AC adjusts the spark timing and/or air-fuel ratio until a local optimum in performance has been reached [8],[9], [10]. Thus, AC differs from conventional automotive engine controls and feedback controls in that it searches for and maintains the optimum setpoint values of the variables under control. These values maximize the engine performance.

(1.3) Adaptive Control

Figure 1 is a block diagram representation of a single level extremum seeking adaptive control system. The objective of such a control system is to identify and maintain the optimum setpoint $X^{\#}$ of the system. This setpoint will maintain the output Z at its extremum (in this case its maximum) value $Z^{\#}$. In this simple system the relationship between the input and the output (the system characteristic) has been assumed to be given by:

$$Z = Z^{\#} - \lambda(X^{\#} - X_o)^2 \qquad (1.3\text{-}1)$$

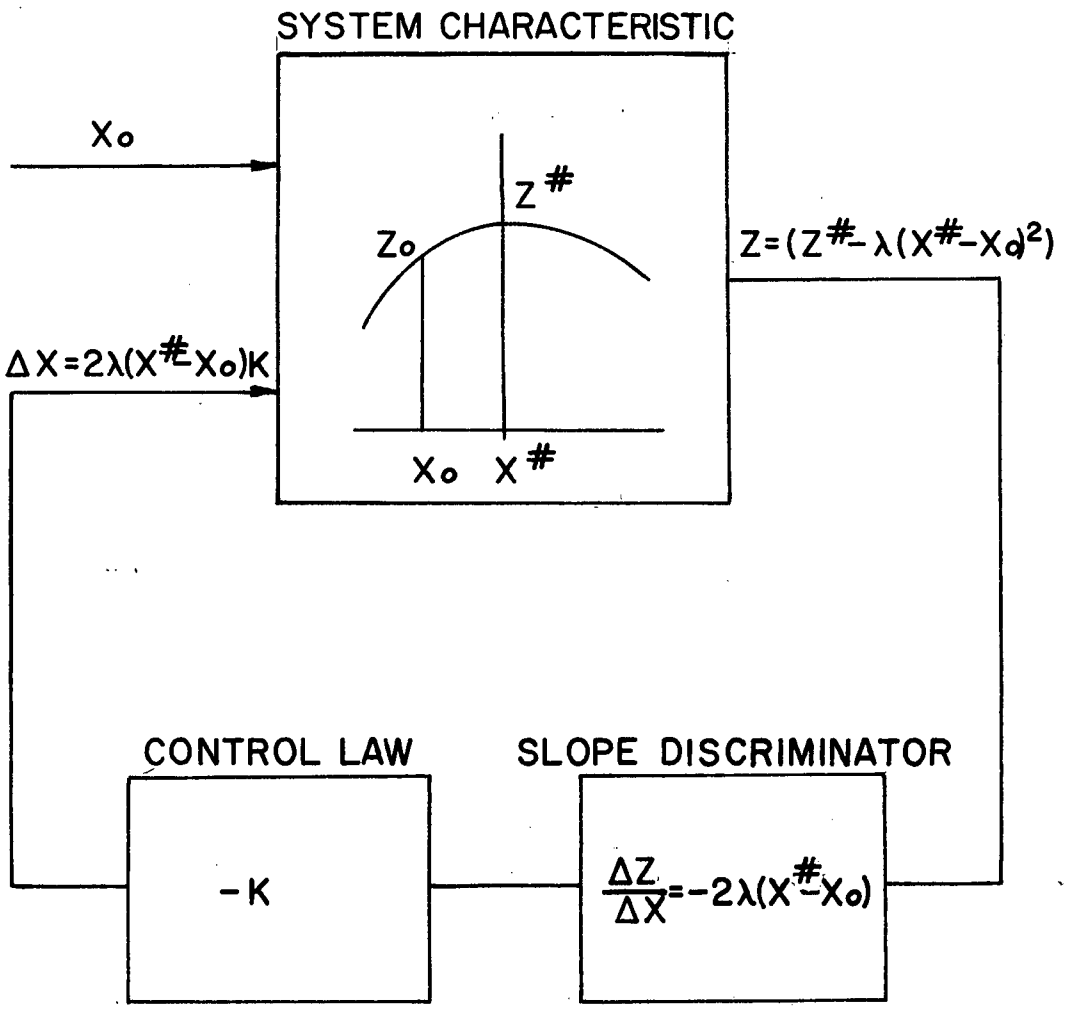

Figure 1: Single Level Extremum Seeking Adaptive Controller

The condition which determines that the optimum is reached occurs when the slope of the system characteristic ($\Delta Z/\Delta X$) becomes zero. For example, if the system is initially at some point X_o away from $X^{\#}$ and the control makes a change to some new X, then a corresponding change in Z will result. The change in output Z is then determined with respect to the change in input X. The resulting signal ($\Delta Z/\Delta X$) is used to drive the system toward the optimum $X^{\#}$ where $\Delta Z/\Delta X$ approaches 0.

The control law (i.e. the law which governs the control response for a given error signal ($\Delta Z/\Delta X$) in Figure 1 is a simple proportional gain K. More sophisticated control laws may prove valuable in improving system stability and response time. Stability refers to the tendency of the system to approach the optimum with a decreasing amplitude of oscillation. If the system were to oscillate with increasing amplitude around the optimum it would be classed as unstable. Response time refers to the time taken for the system to reach the optimum for an initial setpoint an arbitrary distance away from the optimum. For example, derivative control (i.e. control proportional to the rate of change of error) may be applied in conjunction with the proportional control to improve the system response time. A complete discussion of the stability and response time problems is beyond the scope of this work and the interested reader is referred to [16],[17].

An important feature of adaptive control illustrated in Figure 1 is that if there is only one maximum within the operating range then this will be the point the control will seek to operate at. All other points will produce a local gradient $(\Delta Z/\Delta X)$. Thus a control signal $K(\Delta Z/\Delta X)$ will exist and drive the system until $\Delta Z/\Delta X$ becomes zero at a local optimum.

Adaptive control can be easily extended to control two or more variables. Initial small perturbations are made in the setpoints of the variables under control. The effects of these perturbations are then observed. The observations enable the controller to determine the direction in which the inputs are adjusted to achieve the "steepest ascent" toward their optimum setpoints.

(1.4) Application of Adaptive Control to Internal Combustion Engines

Figure 2 illustrates the structure of the controls and dynamics of the engine-vehicle-driver system. The adaptive control supervises the control of several plant variables in response to the driver control of fuel rate.

Figure 3 is a conceptual illustration of an adaptive spark timing controller for an internal combustion engine. The truth table of the And-Nor logic gate of this controller is presented in Table I. The control senses the engine mean torque and spark timing. The two variables are then compared by the

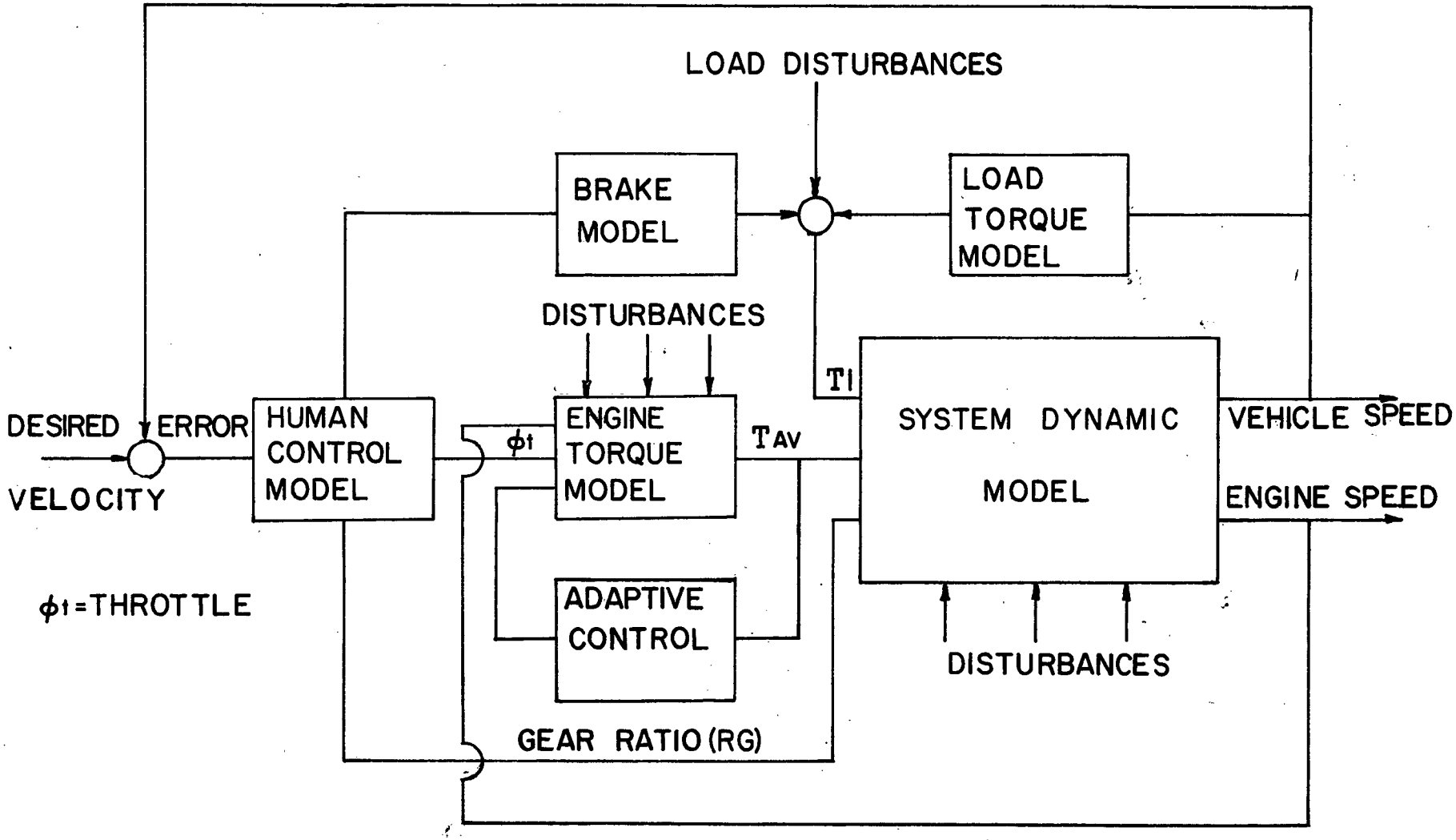

Figure 2: Structure of Controls and Dynamics of the Engine Vehicle Driver System

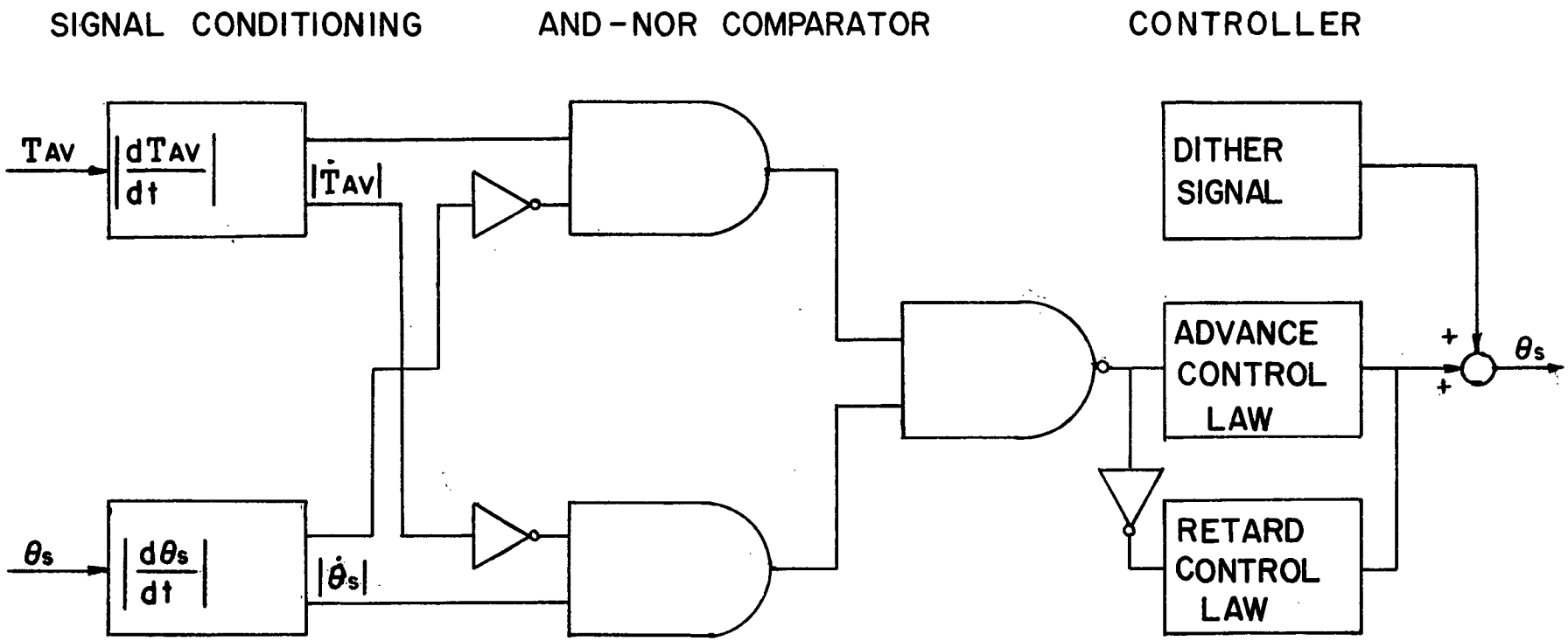

Figure 3: Conceptual Block Diagram of an Adaptive Spark Timing Controller

TABLE I: ADAPTIVE SPARK TIMING CONTROLLER TRUTH TABLE

Torque Signal 0-Decreasing 1-Increasing	Spark Timing 0-Retarding 1-Advancing	Logic Gate Output 0-Retard the Spark 1-Advance the Spark
0	0	1
0	1	0
1	0	0
1	1	1

And-Nor logic gate which activates the appropriate control law. A dither signal, which is merely a small perturbation applied to the control signal, prevents the control from sticking on a false optimum. For example, if the control had initially reached an optimum which because of disturbances has subsequently shifted, the system could not respond without a small dither to push the system off its old, now false optimum.

Figure 4 illustrates the relationship between T_{av} and θ_s correlated for all loads and speeds. The relationship displays the single maximum torque which insures that an adaptive control scheme will achieve the optimum setpoint. Figure 5 illustrates the hypersurface relationship between the four variables T_{av}, W_e, ϕ_T, and θ_s for a typical internal combustion engine. The throttle effect is to shift the three dimensional surface up and down without affecting its shape appreciably. The surface describing a real system is more complex than that of Figure 5 because many more variables are involved. One of the advantages of adaptive control is that it requires no more than a qualitative understanding of this hypersurface. Specifically, as long as only one optimum setpoint exists in the operating range this is a sufficient condition to guarantee the realizability of an adaptive controller.

The effects of disturbances in variables influencing engine operation will in most circumstances affect the location of the optimum spark timing and air-fuel ratio. Thus adaptive

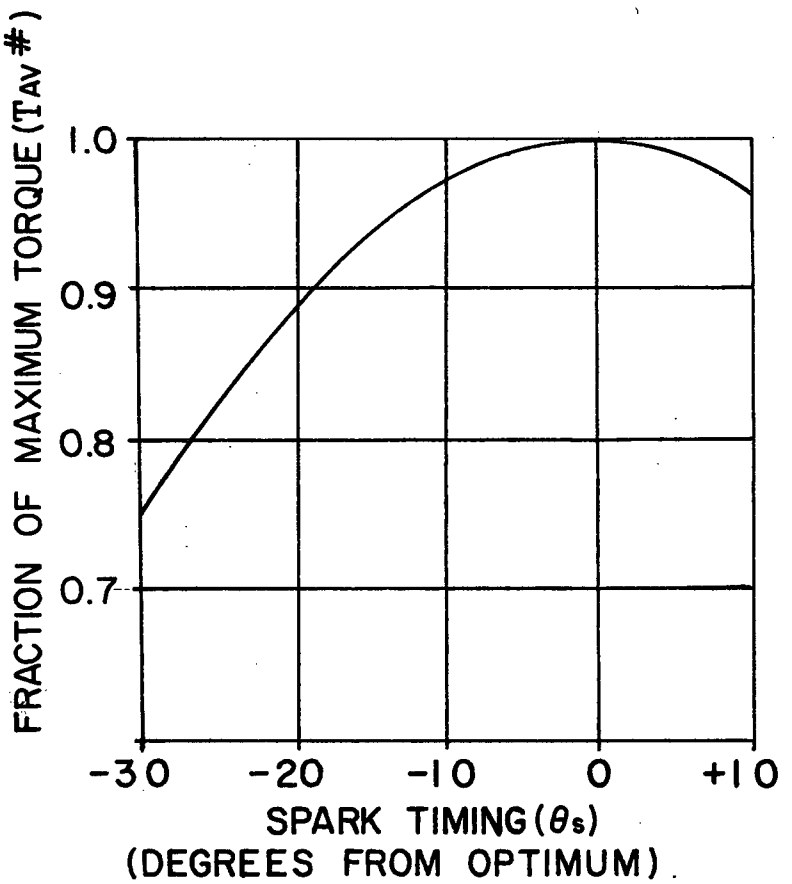

Figure 4: The Effect of Spark Timing on the Mean Torque Output

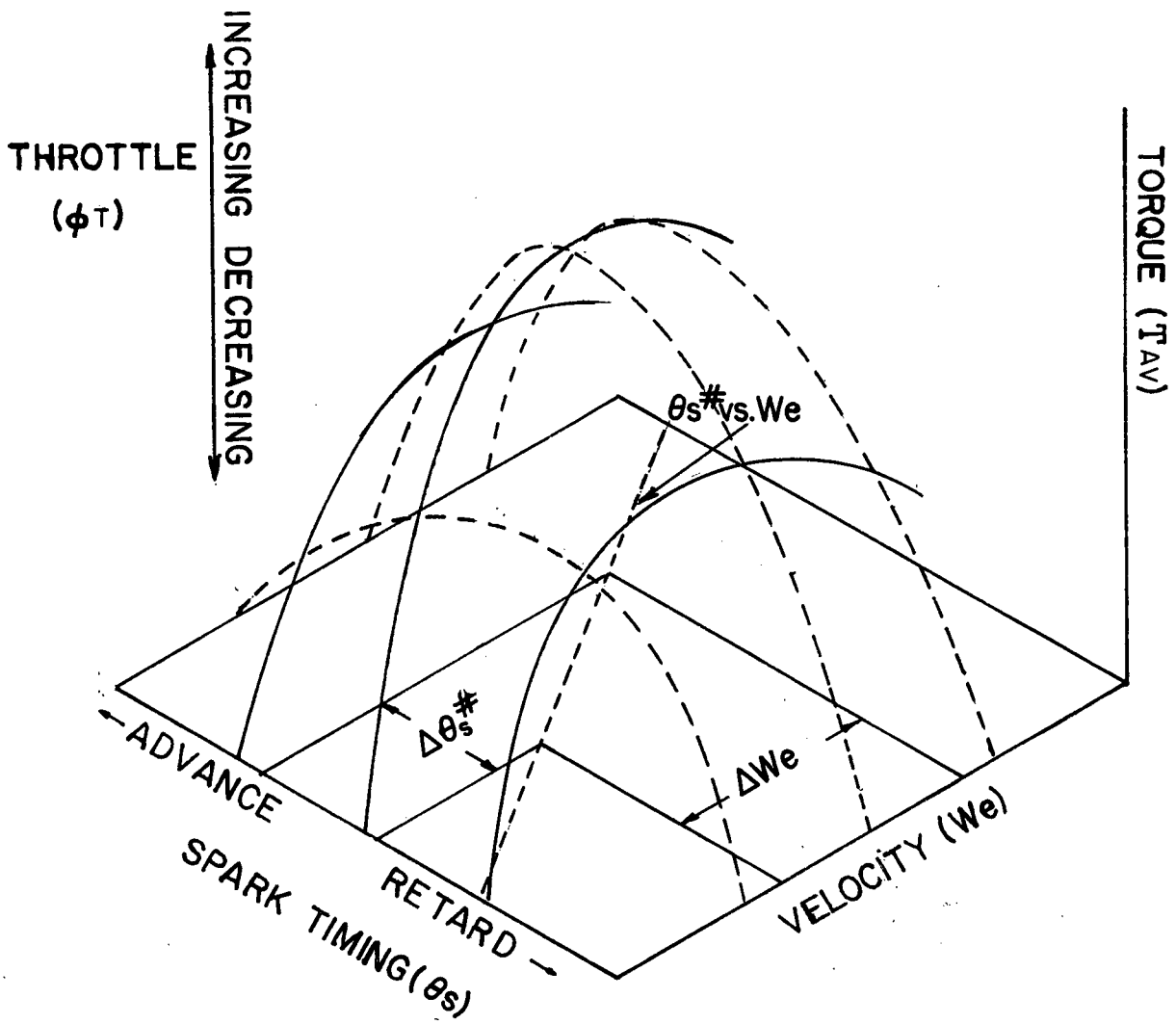

Figure 5: Hypersurface Illustrating the Relationship Between Engine Variables

control will compensate for disturbances in other uncontrolled variables by continuously adjusting the spark timing to its local optimum.

This compensation can be illustrated by considering the result of a change in throttle position. As a result of the change in throttle position a change in engine velocity (ΔWe) will occur as shown in Figure 5. Thus the location of the optimum spark timing $\theta s^{\#}$ will shift by $\Delta\theta s^{\#}$. The controller will sense this shift by observing an increase in the local gradient ($\Delta Tav/\Delta\theta s$). This gradient will drive the system up to its new optimum.

The adaptive control of internal combustion engines depends upon the fact that adjustment of the variables under control will be on the order of only several cycles. Ideally, the control would adjust on a cycle to cycle basis. This fact will require the replacement of the current carburetor and distributor advance units by electronic fuel injection and electronic spark distribution and timing devices. The present carburetor and distributor advance units have response times in the order of many engine cycles. These long responsestimes are caused by delays due to long vacuum and manifold connections. The electronic devices have the capability of readjusting the air-fuel ratio and spark timing on a cycle to cycle basis thus achieving the desired controller response.

The disturbances encountered by the automobile engine ordinarily have long time constants (i.e. the time taken for the disturbed variable to move from its initial value to within 37% of its final value). For example, the disturbances to the optimum spark timing $\theta s^{\#}$ during warmup have time constants in the order of minutes. Other disturbances are caused by acceleration (with time constants determined experimentally to be between 5 and 10 seconds in normal urban driving), aging and wear (time constants on the order of months) and environmental change (time constants on the order of hours). The adaptive controller with its ability to adjust the spark timing and air-fuel ratio on a cycle to cycle basis will have little problem in compensating for these disturbances.

Some disturbances encountered will have very short time constants and may produce large changes in the location of the optimum setpoint. Such disturbances are caused by driving onto ice or going up a steep hill. The system response time to such disturbances is determined by the controller time constant. Careful design of the control law will minimize this response time.

(1.5) Mean Torque Measurement

Several methods of measuring the engine mean torque output are possible. One way is to measure the twist in the crank or driveshaft. This involves bonding strain gauge or variable reluctance transducers to the shaft. Disadvantages of

this method include the space required, the transmission of the signal off the rotating shaft, cost and reliability. Location of this type of system downstream of the flywheel presents problems because of phase lag and attenuation.

A second method of measuring output torque which is used in helicopters consists of a helical gear system. The output shaft of the power plant as well as driving the load also engages a helical gear connected to a hydraulic cylinder and control value. If the output torque of the engine increases, the helical gear causes the control pressure to change, thereby repositioning the fuel control spool. The disadvantages of this system include frequency response, size and cost. The frequency response problem is the chief disadvantage. In the internal combustion engine torque changes occur at a frequency of 150 rad/sec or higher. Preliminary analysis shows that a helical gear system will not respond to changes at this frequency.

A third possibility is to measure the mean torque by observation of motion which is dependent on the mean torque (T_{av}). Such motions include the flywheel acceleration and the relative angle across the clutch (i.e. the displacement of the driven plate relative to the driving plate). These motions could be measured by using suitable magnetic pickups above the flywheelsteeth or notches on the clutch plates. These signals from the magnetic pickups could then be processed in digital

timing and logic circuits to produce the desired control signals. The third possibility is the subject of this work.

(1.6) Preview of Thesis

Section 2 presents the dynamics of the lumped parameter system. The engine torque model and the load torque model are also presented in this section. Section 3 presents the derivation of an equivalent linear system. In Section 4 the equations of motion developed in Section 3 are solved for the general case. Section 5 presents the solutions of Section 4 for a special case. In Section 6 the equations of motion from Section 2 are simulated by the IBM 370 computer for the same special case as in Section 4. A comparison of the analytic and simulated solutions is also made in Section 6. Section 7 evaluates potential observers for T_{av} and Section 8 presents the conclusions of the thesis. Section 9 presents recommendations for future work.

2 DYNAMIC ANALYSIS OF INTERNAL COMBUSTION ENGINE DRIVER VEHICLE SYSTEMS

(2.1) System Dynamics

Figure 6 is a schematic representation of the chief dynamic elements and their arrangement in an idealized lumped parameter engine vehicle system. The chief dynamic elements are; the engine inertia (Je), the clutch spring (Kc), the clutch damper (nonlinear coulomb damping, Tc), the transmission ratio (Rg), the driveshaft spring (Ks), the rear end ratio (R), the tire spring (Kt), the tire damper (Dt) and the vehicle inertia (Jl). The system has six degrees of freedom given by; $\theta_1, \theta_2, \theta_3, \theta_4, \theta_5, \theta_6$. Three external torques act on the system; the engine output torque (Te), the load torque (Tl) and the brake torque (Tb). The dynamic analysis of the system results in the following equations of motion:

$$Te = Je\,\ddot{\theta}_1 + Kc(\theta_1 - \theta_2) + Tc \qquad (2.1\text{-}1)$$

$$T_3 = Rg(Kc(\theta_1 - \theta_2) + Tc) \qquad (2.1\text{-}2)$$

$$\theta_2 = Rg\,\theta_3 \qquad (2.1\text{-}3)$$

$$T_3 = T_4 = Ks(\theta_3 - \theta_4) \qquad (2.1\text{-}4)$$

$$\theta_4 = R\theta_5 \qquad (2.1\text{-}5)$$

$$T_5 = R\,T_4 \qquad (2.1\text{-}6)$$

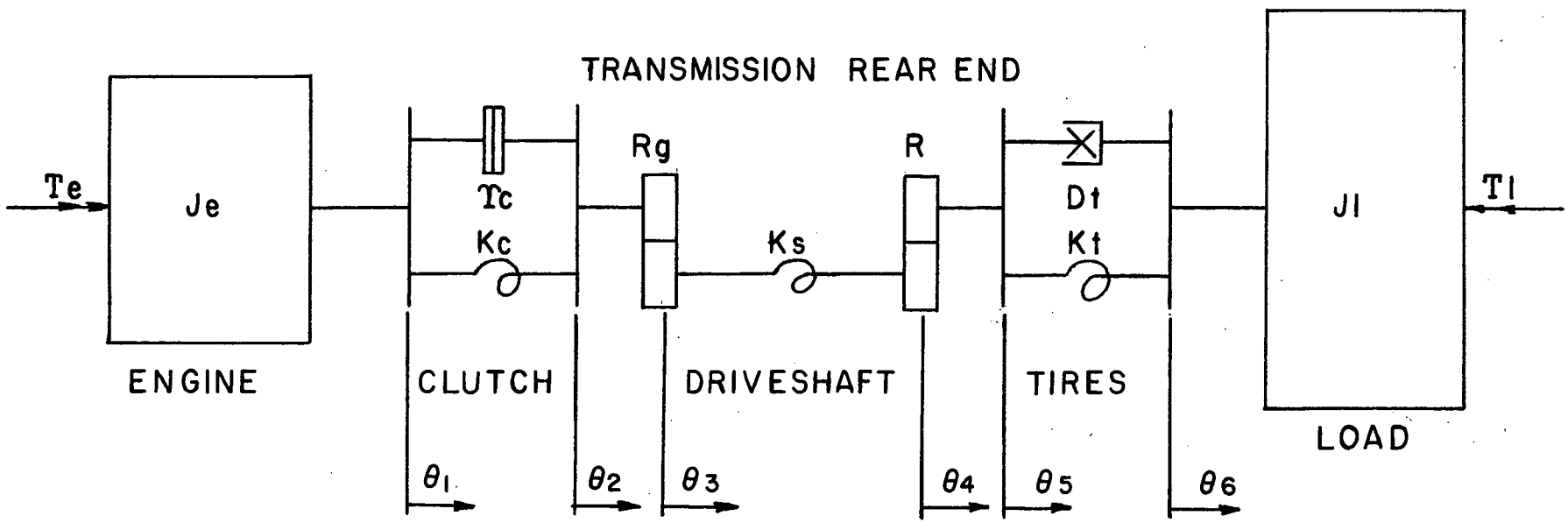

Figure 6: Lumped Parameter Engine Vehicle System

$$T_5 = K_t(\theta_5 - \theta_6) + D_t(\dot{\theta}_5 - \dot{\theta}_6) \qquad (2.1\text{-}7)$$

$$J_l \ddot{\theta}_6 + T_l + T_b = K_t(\theta_5 - \theta_6) + D_t(\dot{\theta}_5 - \dot{\theta}_6) \qquad (2.1\text{-}8)$$

For a detailed analysis and derivation of the system governing equations including assumptions see Appendix I.

(2.2) External Torques

The three external torques acting on the system are examined in this section. Assumptions are made which simplify the expressions for these torques. These simplifications are made so that the resulting model may be easily solved analytically.

(2.2.1) Engine Output Torque (Te)

It is shown in [18] that the instantaneous engine torque T_e for a four stroke cycle engine can be expressed as a Fourier series;

$$\frac{T_e}{T_{av}} = 1 + C_{\frac{1}{2}} \sin\frac{\theta}{2} + C_1 \sin\theta + C_{\frac{3}{2}} \sin\frac{3\theta}{2} + \cdots$$

$$+ B_{\frac{1}{2}} \cos\frac{\theta}{2} + B_1 \cos\theta + B_{\frac{3}{2}} \cos\frac{3\theta}{2} + \cdots \qquad (2.2.1\text{-}1)$$

Here θ is the crank angle ($\theta = W_e t$) and T_{av} is the engine mean

output torque. The coefficients $C_{\frac{1}{2}}, C_1, C_{\frac{3}{2}}, \ldots, B_{\frac{1}{2}}, B_1, B_{\frac{3}{2}}, \ldots,$ are given in [18] for a single cylinder four stroke cycle engine. The analysis will assume constant values for these torque coefficients. In actual engines this is not generally the case as considerable cycle to cycle variation occurs in practice. In future work the model being developed will be used in testing adaptive control schemes. For the later work disturbances in the coefficients can be introduced to simulate the variations when evaluating adaptive control schemes.

For a four cylinder engine (the case of interest in this analysis) the instantaneous output torque is given by summing the torques from individual cylinders. The resulting torque expression is:

$$\frac{Te}{Tav} = 1 + 2C_2\sin 2\theta + 4C_4\sin 4\theta + \cdots + 8B_8\cos 8\theta \qquad (2.2.1\text{-}2)$$

where terms to the eighth order have been included. Terms higher than the eighth order are much smaller and have much less effect on the instantaneous engine torque. For the purpose of the analytic investigation the expression (2.2.1-2) is simplified further to:

$$\frac{Te}{Tav} = 1 + K1\sin(2We)t \qquad (2.2.1\text{-}3)$$

where $K1 = Tmax/Tav = 2.5$ for four cylinder four stroke cycle engines [19] and We/π is the period of the torque fluctuation.

The error between the expression (2.2.1-2) and the expression (2.2.1-3) is illustrated in Figure 7. As shown, the

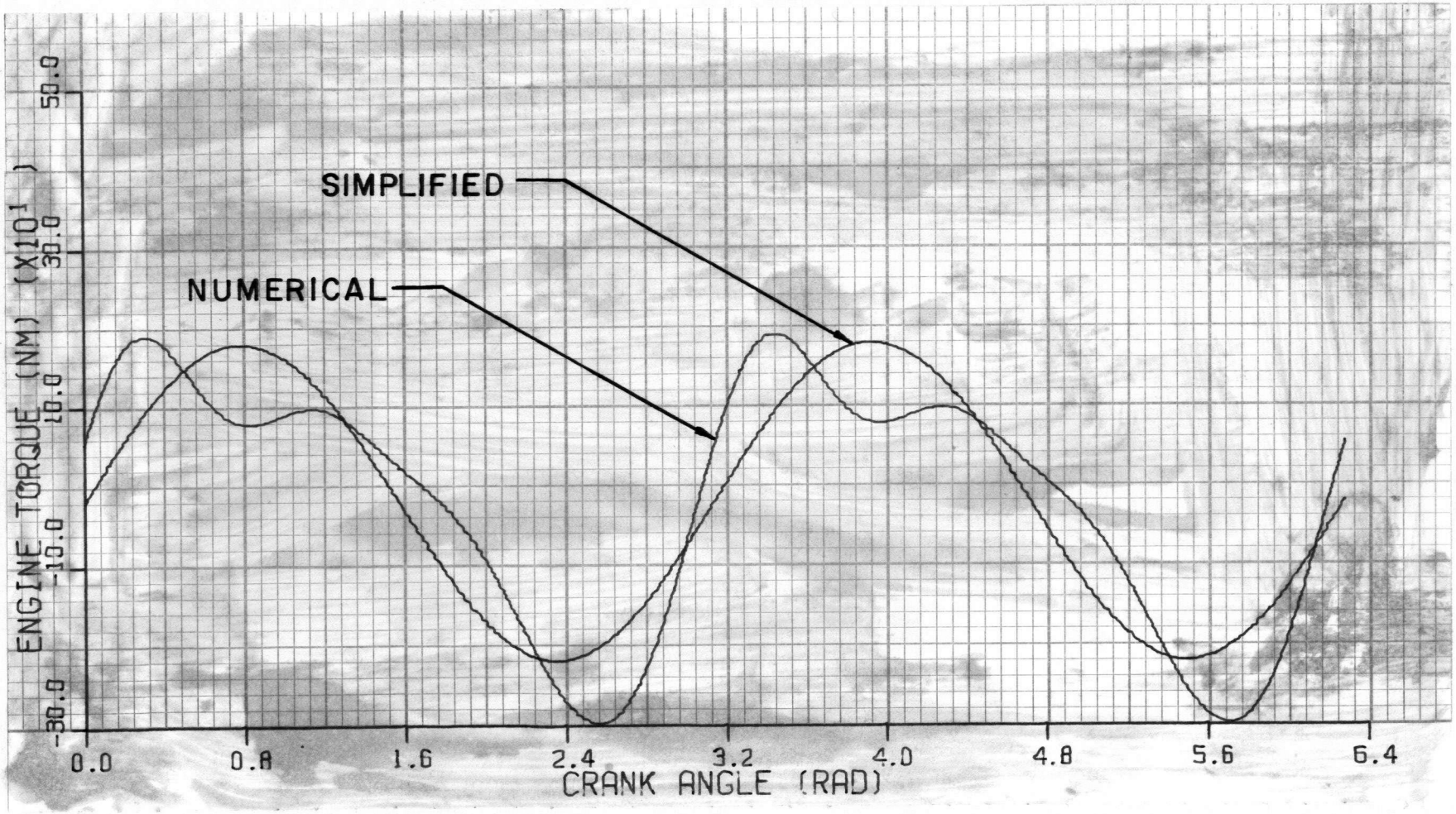

Figure 7: Comparison of the Simplified and Numerical Series Engine Torque Signals

approximation made in equation (2.2.1-3) modifies the energy input timing but maintains approximately the same energy input per cycle.

The factor Tav must be investigated to produce an analytic expression for use in the simulated model. Figure 8 illustrates the relationship between engine speed (We), throttle (ϕt) and mean engine output torque (Tav) for the Ford Cortina 2000 c.c. Engine (which will be the engine to which the analysis will be applied). Recall that Figure 4 presents a similar relationship between spark timing (θs) and mean engine output torque (Tav). Keeping the above relationships in mind a functional relationship of the following form is suggested:

$$Tav = Tav(We, \phi t, \theta s, A/F, \psi, T, P, W, \xi) \qquad (2.2.1\text{-}4)$$

In this relationship A/F is the air-fuel ratio, ψ is the relative humidity, T is the ambient air temperature, P is the ambient air pressure, W is the engine wear (age), and ξ is to account for other factors. In this analysis all effects other than those of speed (We), throttle (ϕt) and spark timing (θs) will be ignored. Equation (2.2.1-4) then reduces to:

$$Tav = Tav(We, \phi t, \theta s) \qquad (2.2.1\text{-}5)$$

To evaluate (2.2.1-5) it is noted that in Figure 8 for a fixed throttle position there exists a maximum torque ($Tavmax$) which occurs at a particular velocity ($We^{\#}$). Both

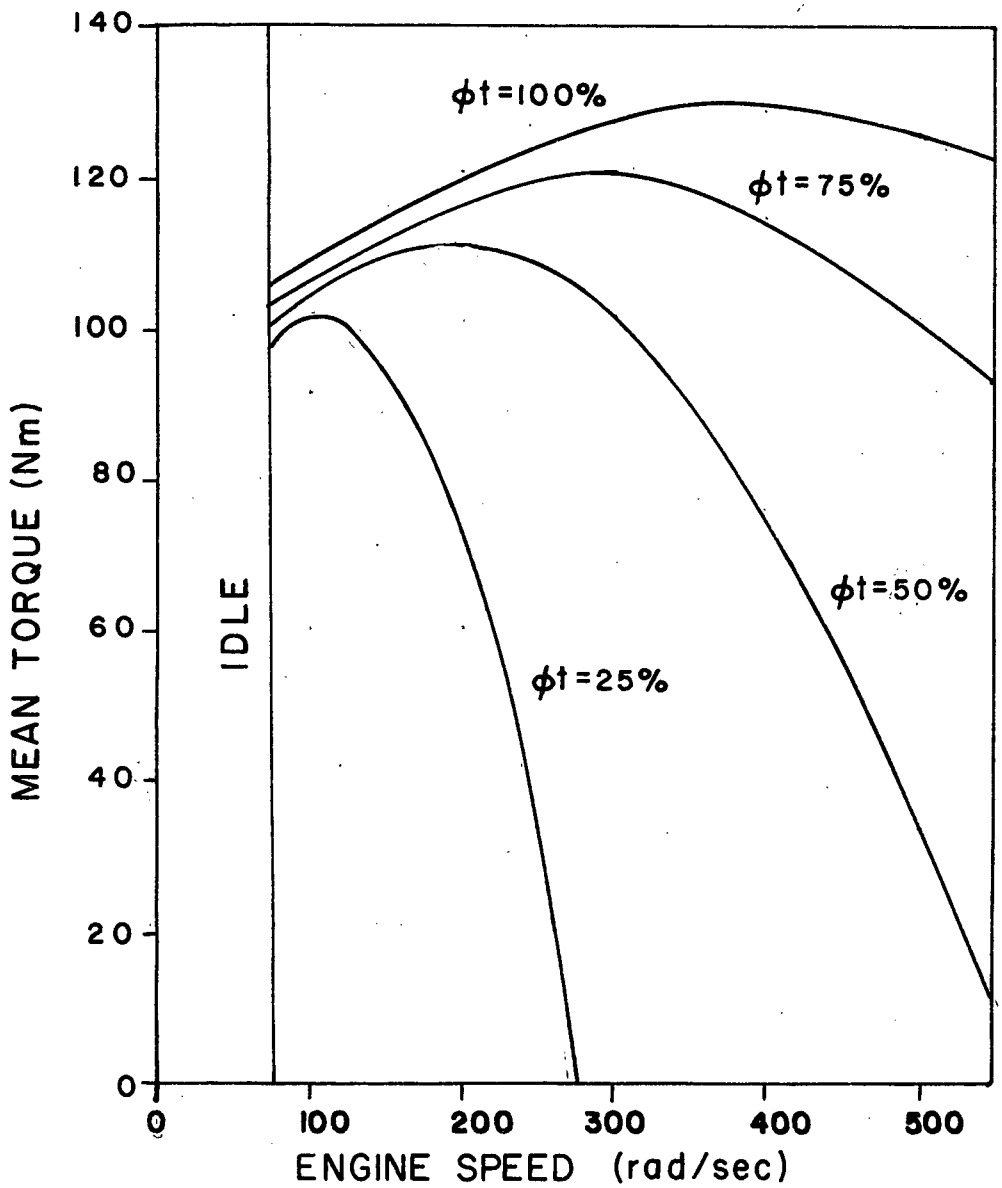

Figure 8: Mean Torque of the Cortina 2000 c.c. Engine

of these variables then are functions of throttle (ϕt) alone, or:

$$Tavmax = Tavmax(\phi t) \qquad (2.2.1\text{-}6)$$

$$We^{\#} = We^{\#}(\phi t) \qquad (2.2.1\text{-}7)$$

In the case of the Cortina 2000 c.c. engine they have been evaluated by making plots of $Tavmax$ vs ϕt and $We^{\#}$ vs ϕt. The following relationships result:

$$Tavmax = 93.4 + 0.355 \times \phi t \quad (Nm) \qquad (2.2.1\text{-}8)$$

$$We = 3.86 \times \phi t \quad (rad/sec) \qquad (2.2.1\text{-}9)$$

Assuming the relationship between Tav and We to be parabolic in nature the following equation may be written:

$$Tav(\phi t, We) = Tavmax \left[1 - CWe\left\{\frac{We}{We^{\#}} - 1\right\}^2\right] \qquad (2.2.1\text{-}10)$$

This leaves one remaining constant CWe which has to be evaluated from Figure 8. The result of this evaluation is:

$$CWe = 0.275 \qquad (2.2.1\text{-}11)$$

The other factor, the spark timing, is analyzed in the same fashion as the throttle. The first step is determining the spark timing at which the maximum torque occurs. In this analysis it is treated as a function of speed alone:

$$\theta s^{\#} = \theta s^{\#}(\phi t) \qquad (2.2.1\text{-}12)$$

From data for the Cortina 2000 c.c. engine, it is found that:

$$\theta s^{\#} = (1.48 \times 10^{-2}) We \quad \text{(Degrees BTDC)} \qquad (2.2.1\text{-}13)$$

With this equation and remembering Figure 4, the following relationship is proposed:

$$Tav(\theta s) = Tav(\phi t, We)\left[1 - C_{1ST}(\theta s - \theta s^{\#}) - C_{2ST}(\theta s - \theta s^{\#})^2\right] \qquad (2.2.1\text{-}14)$$

where $C_{1ST} = 1.246 \times 10^{-4}$ and $C_{2ST} = 3.684 \times 10^{-3}$

From the preceding paragraphs the engine mean torque (Tav) is given by:

$$Tav = Tavmax\left[1 - CWe\left\{\frac{We}{We^{\#}} - 1\right\}^2\right]\left[1 - C_{1ST}(\theta s - \theta s^{\#}) - C_{2ST}(\theta s - \theta s^{\#})^2\right] \qquad (2.2.1\text{-}15)$$

(2.2.2) Load Torque (Tl)

As shown in Figure 2 the load on a vehicle results from three separate forces; the aerodynamic drag force, the rolling resistance force and the gradient force. An examination of these three forces follows. An expression for the load torque (Tl) is derived from these forces.

(2.2.2.1) Aerodynamic Drag Force (Df)

The aerodynamic drag force may be calculated from the well known relationship:

$$Df = \frac{1}{2} \rho V^2 \times C_{DO} A_p \qquad (2.2.2.1\text{-}1)$$

In this relationship C_{DO} is the drag coefficient taken as 0.45 (typical of modern streamlined vehicles), A_p is the vehicle projected area (which is $1.53 m^2$ for the Cortina sedan) and $\frac{\rho V^2}{2}$ is the dynamic pressure (where ρ is the air density (1.23 N sec^2/m^4) and V is the relative velocity of the air). This results in the following expression for the aerodynamic drag:

$$Df = 0.424 \times V^2 \quad (N) \qquad (2.2.2.1\text{-}2)$$

where V is in m/sec.

(2.2.2.2) Rolling Resistance Force (Rf)

As shown in [20] the rolling resistance force is given by:

$$Rf = Kr \times Wt \qquad (2.2.2.2\text{-}1)$$

where Kr is an empirical constant giving the rolling resistance due to mechanical friction, tire inflation and the aerodynamic and pumping effects in the tires in (N drag)/(N vehicle weight). The constant is given as:

$$Kr = 0.005 + \frac{1.04 \times 10^3}{P} + \frac{1.21 \times V^2}{P} \qquad (2.2.2.2\text{-}2)$$

where P is the tire inflation pressure in Pascals and V is the vehicle velocity in m/sec. Consulting Table II, $p = 1.66 \times 10^5$ (Pa) and Kr becomes:

$$Kr = 0.01126 + 7.3 \times 10^{-6} V^2 \qquad (2.2.2.2\text{-}3)$$

TABLE II: PHYSICAL CONSTANTS OF THE CORTINA 200 c.c. SEDAN

Quantity	Symbol	Value	Units
Engine Inertia	Je	01136	$Nmsec^2/rad$
Load Inertia	Jl	102	$Nmsec^2/rad$
Clutch Spring	Kc	1500	Nm/rad
Driveshaft Spring	Ks	7800	Nm/rad
Tire Spring	Kt	6950	Nm/rad
Clutch Damper	Tc		
Dynamic		$\pm$3.2	Nm
Static		$\pm$6.0	Nm
Linearized Clutch Damping	Dc	3.8	Nmsec/rad
Tire Damper	Dt	58.0	Nmsec/rad
Vehicle Weight	Wt	1100	N
Frontal Area	Ap	1.53	m^2
Tire Inflation Pressure	p	1.66×10^5	Pa (N/m^2)
Dynamic Wheel Radius	Rw	0.3	m
Rear End Ratio	R	3.44	
Gear Ratios	Rg		
1st		3.65	
2nd		1.97	
3rd		1.37	
4th		1.00	

Again consulting Table II and finding Wt=11100 (N) (the vehicle weight) the final result for Rf can be given:

$$Rf = Kr \times Wt = 125 + 0.0809 \times V^2 \quad (N) \qquad (2.2.2.2\text{-}4)$$

(2.2.2.3) Gradient Drag Force (Gf)

The increase (or decrease) in load experienced by a vehicle climbing (or descending) a gradient is given by the familiar expression:

$$Gf = Wt \times \sin\theta i \qquad (2.2.2.3\text{-}1)$$

where θi is the incline angle. Therefore, the expression (2.2.2.3-1) can be written:

$$Gf = 11100 \times \sin\theta i \quad (N) \qquad (2.2.2.3\text{-}1)$$

(2.2.2.4) Combination of the Load Force

Figure 9 is a free body diagram illustrating the three forces acting on the vehicle. Therefore, the total force acting against the vehicle becomes:

$$Fl = Df + Rf + Gf \qquad (2.2.2.4\text{-}1)$$

which shows up as an external torque (Tl) at the rear wheels:

$$Tl = Fl \times Rw \qquad (2.2.2.4\text{-}2)$$

In the expression (2.2.2.4-2) Rw is the wheel radius which is given as 0.3 meters in Table II. As well V can be replaced by:

$$V = Rw \times \dot{\theta}6 \qquad (2.2.2.4\text{-}3)$$

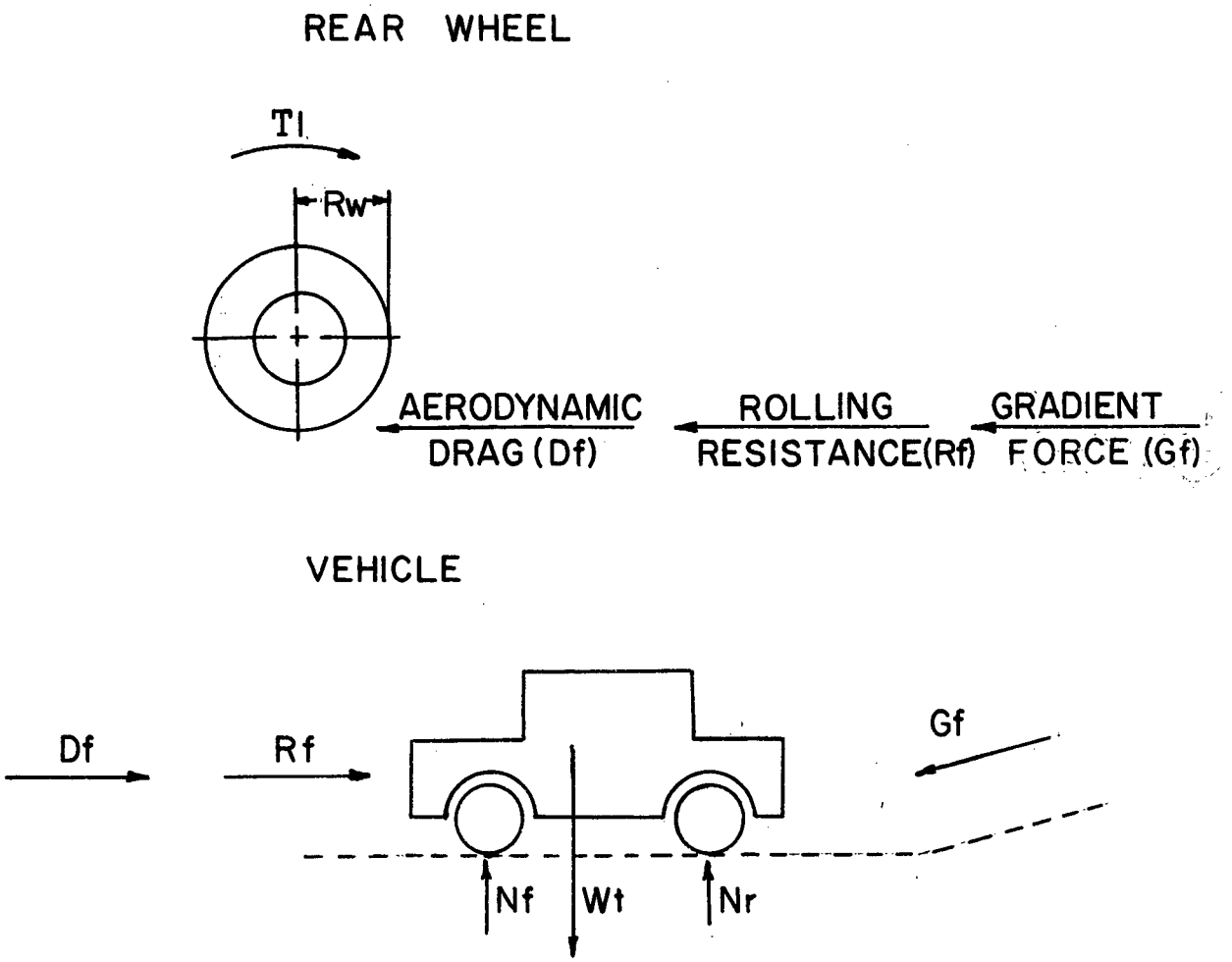

Figure 9: Free Body Diagram Illustrating the External Forces on a Vehicle

which results in:

$$Tl = 37.5 + 1.52\times10^{-2}(\dot{\theta}6)^2 + 3.32\times10^{3}(\sin\theta i) \quad (Nm) \qquad (2.2.2.4\text{-}4)$$

The first two terms of (2.2.2.4-4) are plotted in Figure 10 for a normal range of operating speeds. The effect of the third term is illustrated by the shifting of the plotted curve upward as indicated in Figure 10.

The relationship of (2.2.2.4-4) is nonlinear. The analysis can be simplified by introducing the concept of an operating point $(Tl^0, \dot{\theta}6^0)$. That is, a point at which the system is in equilibrium operation as shown in Figure 10. If a linear impedance of the form:

$$Z = \frac{d(\text{potential})}{d(\text{flow})} = \frac{dTs^0}{d\dot{\theta}6^0} \qquad (2.2.2.4\text{-}5)$$

is introduced where Ts is the torque from the second term of (2.2.2.4-4). The equation (2.2.2.4-5) may then be written:

$$Ts = 1.52\times10^{-2}\,\dot{\theta}6^2 \approx 1.52\times10^{-2}(\dot{\theta}6^0)^2 + 3.04\times10^{-2}\dot{\theta}6^0(\dot{\theta}6 - \dot{\theta}6^0) \quad (Nm) \qquad (2.2.2.4\text{-}6)$$

for small perturbations $(\dot{\theta}6 - \dot{\theta}6^0)$ around the operating point.

The third term of (2.2.2.4-4) may be linearized by recognizing that θi will generally be small $(<5^0)$ and therefore the small angle approximation can be made to obtain:

$$Tg = 3.32\times10^{3}(\theta i) \qquad (2.2.2.4\text{-}7)$$

where θi is in radians.

Therefore, the final expression for the load torque (Tl) linearized about an operating point $(Tl^0, \dot{\theta}6^0)$ is:

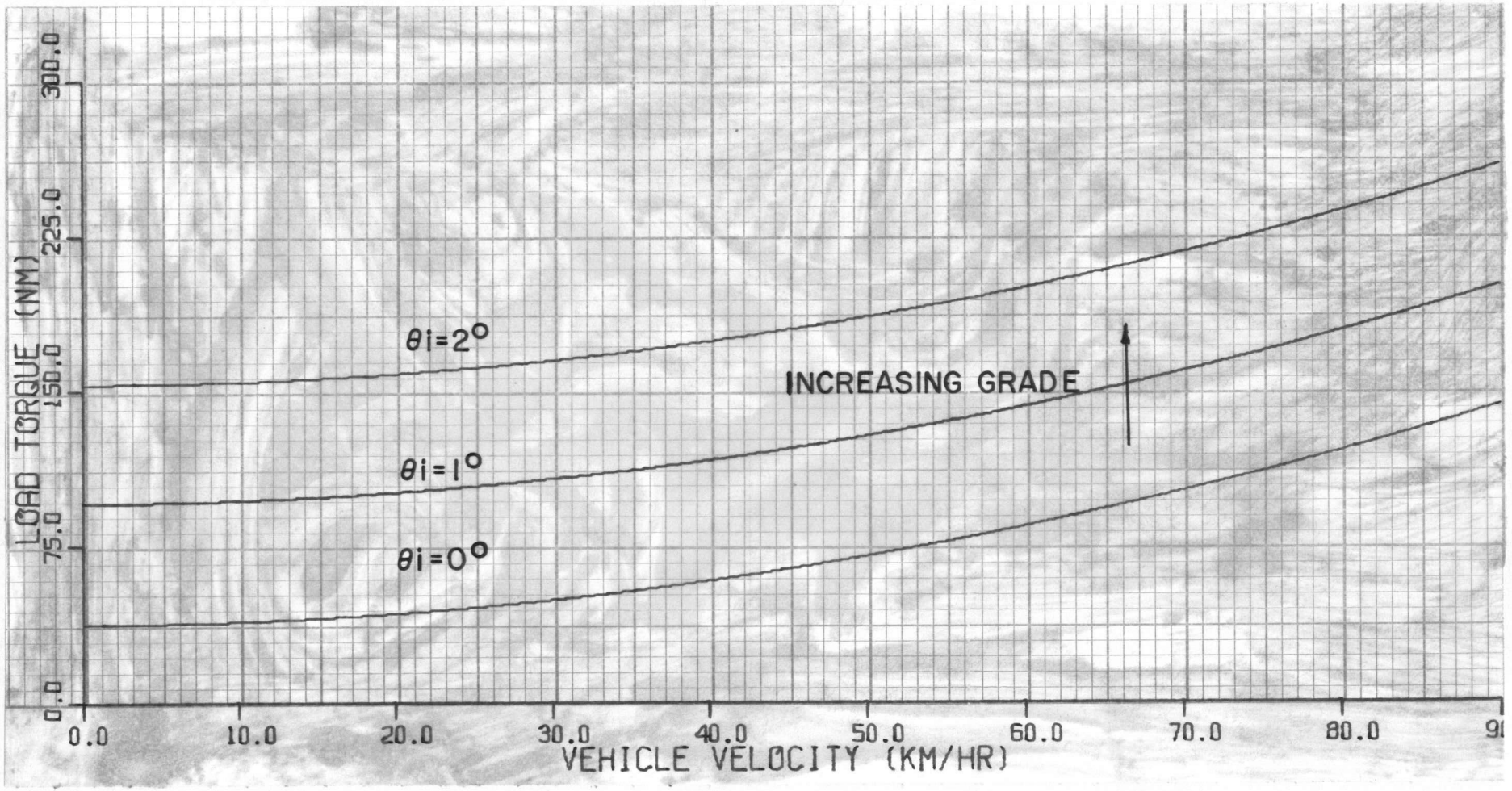

Figure 10: Load Torque on the Cortina Sedan

$$Tl = 37.5 + 1.52 \times 10^{-2}(\dot{\theta}6^{0}) + 3.04 \times 10^{-2}(\dot{\theta}6^{0})(\dot{\theta}6 - \dot{\theta}6^{0}) + 3.32 \times 10^{3}(\theta i) \qquad (2.2.2.4\text{-}8)$$

(2.2.3) Brake Torque (Tb)

The brake torque can be thought of as an increase in the load torque which occurs as a result of the driver's desire to slow down. The simplest model for the brake torque can be given by the expression:

$$Tb = BCI \times Tbmax \qquad (2.2.3\text{-}1)$$

Here BCI is a brake command input (percent of maximum possible brake action). Tb represents the brake torque applied which is a fraction of the maximum available brake torque, Tbmax. The expression (2.2.3-1) assumes the brake action is linear.

3 AN EQUIVALENT LINEAR SYSTEM

The system described by equations (2.1-1) to (2.1-8) and Figure 6 is a six degree of freedom system which is cumbersome to analyze analytically. Variables downstream of θ_1 will experience attenuation and phase shifts in the affects caused by T_{av}. Thus it is desirable to focus primary attention on θ_1 and its relationship to T_{av}. Therefore, by replacing the more complicated system of Figure 6 by the equivalent linearized system of Figure 11 the analysis can be considerably simplified without eliminating the important information. The validity of this simplification is established later by computer simulation of the system of Figure 6 and comparing the results with those obtained from the analytic investigation of Figure 11.

(3.1) A Constant Speed System

The first step in the derivation of the equivalent system of Figure 11 is to eliminate both the transmission and rear end ratios. All components of the resulting system will rotate at the same speed (the engine speed (W_e)). The elimination of the transmission and rear end is accomplished by making the following substitutions:

$$\theta_6' = \theta_6 \times R \times R_g \qquad (3.1\text{-}1)$$

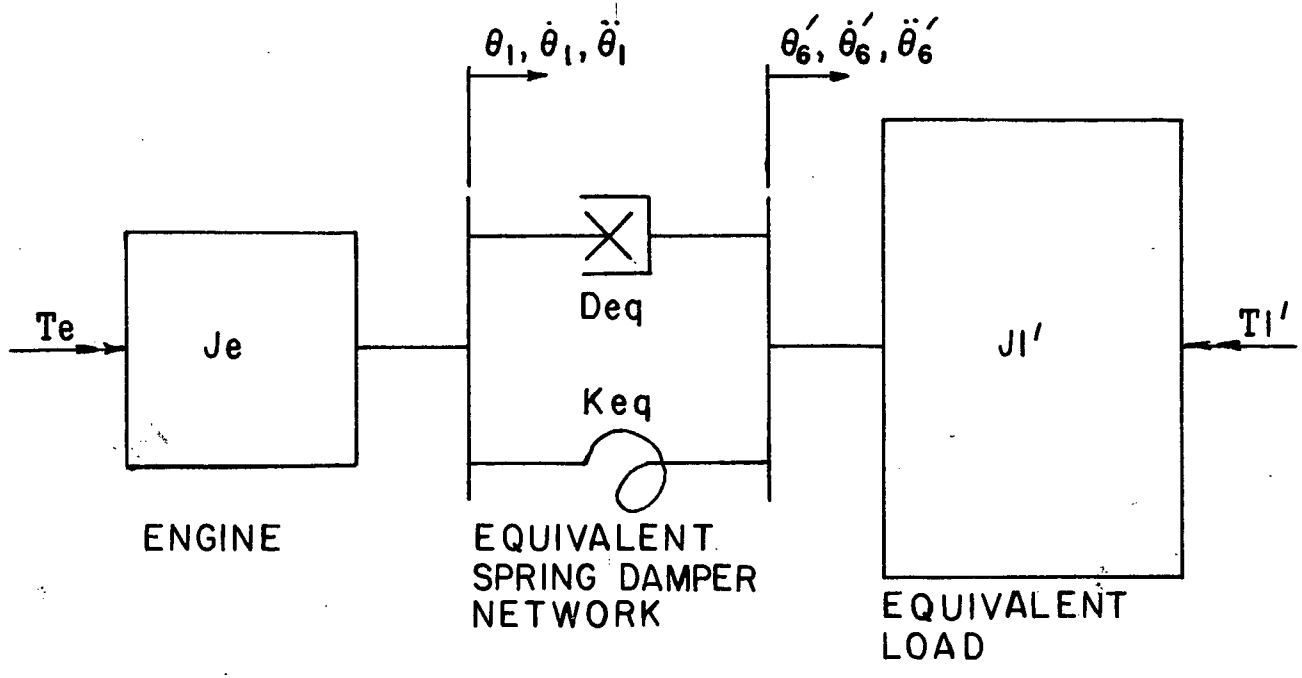

Figure 11: Equivalent Linear Engine Vehicle System

$$Tl' = \frac{Tl}{R(Rg)} \qquad (3.1\text{-}2)$$

$$Jl' = \frac{Jl}{(R(Rg))^2} \qquad (3.1\text{-}3)$$

$$Kt' = \frac{Kt}{(R(Rg))^2} \qquad (3.1\text{-}4)$$

$$Dt' = \frac{Dt}{(R(Rg))^2} \qquad (3.1\text{-}5)$$

$$Ks' = \frac{Ks}{Rg^2} \qquad (3.1\text{-}6)$$

(3.2) Equivalent Spring and Damper

The next step is to replace the spring-damper network between $\theta 1$ and $\theta 6$ by a single equivalent spring (**Keq**) and a single equivalent damper (**Deq**). This can be done by first recognizing:

$$Te - Je\,\ddot{\theta}1 = Tl \qquad (3.2\text{-}1)$$

and

$$Tl' + Jl'\ddot{\theta}6' = T6' = Tl \qquad (3.2\text{-}2)$$

where the components are all rotating at the same speed. The displacement across the clutch, driveshaft and tire ($\theta 1 - \theta 6'$) is:

$$(\theta_1-\theta_6')=\frac{T_1}{Kc}+\frac{T_1}{Ks'}+\frac{T_1}{Kt'} \quad \text{or} \tag{3.2-3}$$

$$(\theta_1-\theta_6')=\frac{T_1}{Keq} \tag{3.2-4}$$

Using (3.2-3) and (3.2-4) the following result is obtained:

$$Keq=\frac{KcKs'Kt'}{(KcKs'+Ks'Kt'+KcKt')} \tag{3.2-5}$$

The first step in combining the clutch damper (Tc) and the equivalent tire damper (Dt') is to replace the nonlinear clutch damper with an equivalent linear one. The method is described in [21] and the results are presented here. The equivalent linear damper (Dc) for the coulomb damped clutch is given by:

$$Dc=\frac{4\times Tc}{\pi W\times \theta_o} \tag{3.2-6}$$

In this equation Tc is the coulomb damping torque which is given in Table I as ± 3.2 (Nm) and W is the frequency of the torque signal (which is twice the engine frequency ($2We$)). θ_o is the amplitude of $(\theta_1-\theta_2)$ and is given by:

$$\theta_o=\frac{TavKl}{Kc}\times\frac{\sqrt{1-\left(\frac{4Tc}{\pi TavKl}\right)^2}}{1-\left(\frac{W}{Wn}\right)^2} \tag{3.2-7}$$

In equation (3.2-7) Wn is the natural frequency of the clutch which is given by:

$$Wn=\sqrt{\frac{Kc}{Jeq}} \tag{3.2-8}$$

where Jeq is the equivalent system inertia. For this two inertia system, Jeq is given by:

$$Jeq = \frac{JeJl'}{Je+Jl'} \tag{3.2-9}$$

Having arrived at the equivalent linear clutch damping the equivalent system damping can be found. The difference between the rotational speeds of the engine and the load $(\dot{\theta}1-\dot{\theta}6')$ must be dissipated in the network between these two elements. Therefore:

$$(\dot{\theta}1-\dot{\theta}6') = \frac{Tl}{Dc} + \frac{Tl}{Dt'} \quad \text{or} \tag{3.2-10}$$

$$(\dot{\theta}1-\dot{\theta}6') = \frac{Tl}{Deq} \tag{3.2-11}$$

From equations (3.2-10) and (3.2-11) the expression for the equivalent system damping Deq is:

$$Deq = \frac{DcDt'}{Dc+Dt'} \tag{3.2-12}$$

(3.3) Equations of Motion of Equivalent Linear System

Having completed the above analysis the equations of motion of Figure 11 can be written:

$$Je\ddot{\theta}1 + Deq(\dot{\theta}1-\dot{\theta}6') + Keq(\theta 1-\theta 6') = Tav(1+Kl\times\sin(2We)t) = Te \tag{3.3-1}$$

$$Jl'\ddot{\theta}6' + Tl' = Deq(\dot{\theta}1-\dot{\theta}6') + Keq(\theta 1-\theta 6') \tag{3.3-2}$$

4 SOLUTION OF THE EQUIVALENT LINEAR SYSTEM

The solutions of equations (3.3-1) and (3.3-2) will consist of three parts; the homogeneous (transient) part, and two particular parts. The particular parts are a constant solution and a sinusoidal solution. A detailed analysis of the solutions is presented in Appendix II and the results are given here.

(4.1) The Transient Response

The solution of the homogeneous equations of motion provides the transient response. For the system of Figure 11 the transient response is given by:

$$\theta_{C1} = e^{-p\tau}(A\cos q\tau + B\sin q\tau) \tag{4.1-1}$$

$$\theta_{C6'} = e^{-p\tau}\left[\frac{\theta_{A6'}}{\theta_{A1}}\right](A\cos q\tau + B\sin q\tau) \tag{4.1-2}$$

In these equations q is the damped natural frequency and p is the negative exponent of decay. These two variables are given by:

$$q = W_n\sqrt{1-(\zeta)^2} = W_d \tag{4.1-3}$$

$$p = \zeta W_n \tag{4.1-4}$$

where ζ is the damping ratio and Wn is the undamped natural frequency. ζ and Wn are given by:

$$\zeta = \frac{Deq}{Dcr} \tag{4.1-5}$$

$$Wn = \sqrt{\frac{Keq}{Jeq}} \tag{4.1-6}$$

where Dcr is the critical damping coefficient given by:

$$Dcr = 2\sqrt{JeqKeq} \tag{4.1-7}$$

A and B are arbitrary constants which are determined from the system boundary conditions. For example, for a step change in mean torque (ΔTav) the boundary conditions can be given by:

$$\theta c1 = \frac{\Delta Tav}{Keq} \qquad (\tau = 0) \tag{4.1-8}$$

$$\dot{\theta}c1 = 0 \qquad (\tau = 0) \tag{4.1-9}$$

$\tau = 0$ when $t = t'$ and t' is the time when the disturbance exciting the transient occurs.

(4.2) The Constant Response

The constant response is given by the following equations:

$$\alpha eng = \ddot{\theta}ssc1 = \ddot{\theta}ssc6' = \frac{Tav - Tlc'}{Je + Jl'} \tag{4.2-1}$$

$$Weng = \dot{\theta}ssc1 = \dot{\theta}ssc6' = Wengi + \int \alpha eng \, d\tau \tag{4.2-2}$$

$$\theta eng = \theta ssc1 = \theta eng1 + \int Weng\, d\tau \qquad (4.2\text{-}3)$$

$$\psi = (\theta ssc1 - \theta ssc6') = \frac{Tav}{Keq} - \frac{Je(Tav - Tlc')}{Keq(Je + Jl')} \qquad (4.2\text{-}4)$$

In the special case where $\alpha eng = 0$ the results (4.2-2) to (4.2-4) reduce to:

$$Weng = constant \qquad (4.2\text{-}5)$$

$$\theta eng = \theta ssc1 + Weng\,(\tau) \qquad (4.2\text{-}6)$$

$$\psi = \frac{Tav}{Keq} \qquad (4.2\text{-}7)$$

(4.3) The Oscillatory Response

The oscillatory response of the system is of the form:

$$\theta sso1 = K1\, Tav \sqrt{\frac{C1^2 + D1^2}{E1^2 + F1^2}}\ \sin(2We t - \Psi 1) \qquad (4.3\text{-}1)$$

$$\theta sso6' = K1\, Tav \sqrt{\frac{C6^2 + D6^2}{E6^2 + F6^2}}\ \sin(2We t - \Psi 6') \qquad (4.3\text{-}2)$$

In these solutions $C1, C6, D1, D6, E1, E6$ and $F1, F6$ are dependent upon the system constants. For a more complete explanation of this solution see Appendix II. The phase angle Ψ is given by:

$$\Psi 1 = \tan^{-1}\left[\frac{G1}{H1}\right] \qquad (4.3\text{-}3)$$

$$\Psi 6' = \tan^{-1}\left[\frac{G6}{H6}\right] \qquad (4.3\text{-}4)$$

(4.4) The Total Response

The total response of the system can be calculated by summing algebraically the responses given in Sections (4.1) to (4.3). This is possible because of the linear nature of the system described by equations (3.3-1) and (3.3-2). For example the total solution for θ_1 is given by summing equations (4.1-1), (4.2-3) and (4.3-1) to yield:

$$\theta_1 = e^{-p\tau}(A\cos q\tau + B\sin q\tau) + \theta_{eng_i} + \int W_{eng}\, d\tau + \qquad (4.4\text{-}1)$$

$$K_1 T_{av} \sqrt{\frac{C_1^2 + D_1^2}{E_1^2 + F_1^2}} \sin(2We\,t - \Psi_1)$$

5 SOLUTIONS OF A SPECIAL CASE

(5.1) The Vehicle Considered

The analysis of Sections 3 and 4 is now applied to a typical small car system. The system selected was a Ford Cortina automobile. The reason for this choice is that this vehicle is typical of modern compact car design. Table II presents the physical constants for the 2000 c.c. engine Cortina Sedan. Appendix III presents the derivation and determination of these constants. The analysis can be easily extended to other vehicles and engines by substitution of the appropriate physical constants and torque signals, equation(2.2.1-3), for those used in this analysis.

(5.2) The Particular Case Considered

For the equivalent system of Figure 11 and equations (3.3-1) and (3.3-2), the solutions (4.1-1) and (4.1-2), (4.2-1), (4.2-2), (4.2-3) and (4.2-4), (4.3-1) and (4.3.2) are determined for a particular case for later comparison purposes with a computer simulation of the system of Figure 6 and equations (2.1-1) to (2.1-8). The particular case investigated is an initial engine speed for 280 rad/sec (~2800 rpm), in third gear (R_g=1.37) producing a 23.5 Nm mean torque (18.5% of maximum output torque). A 10% step change in throttle position is then made resulting in

a new mean output torque of 80 Nm (62% of maximum output torque). The system response to this step change is presented below.

(5.3) The Transient Response

Consulting Table II and using equations (4.1-3), (4.1-4), (4.1-5), (4.1-6), (4.1-7) the following results are obtained:

$$Wn = \sqrt{\frac{Keq}{Jeq}} = 42.4 \text{ (rad/sec)} \tag{5.3-1}$$

$$\zeta = \frac{Deq}{Dcr} = \frac{Deq}{2\sqrt{JeqKeq}} = 0.087 \tag{5.3-2}$$

$$Wnd = Wn\sqrt{1-\zeta^2} = 42.2 \text{ (rad/sec)} \tag{5.3-3}$$

Using these results in equations (4.1-1) and (4.1-2) the following solutions can be written:

$$\theta c1 = e^{-3.68\tau}(A\cos 42.2\tau + B\sin 42.2\tau) \tag{5.3-4}$$

$$\theta c6' = e^{-3.68\tau}D(A\cos 42.2\tau + B\sin 42.2\tau) \tag{5.3-5}$$

The constant D can be evaluated by the method illustrated by equations (AII.3-11) and (AII.3-12). The other two constants A and B are evaluated by consideration of the boundary conditions which are the same as those given by (4.1-8) and (4.1-9).

The evaluation of these constants produces the following set of results:

$$\theta_{c1} = -e^{-3.68\tau}(2.49\times10^{-1}\cos 42.2\tau + 2.09\times10^{-2}\sin 42.2\tau) \quad (5.3\text{-}6)$$

$$\dot{\theta}_{c1} = e^{-3.68\tau}(9.80\sin 42.2\tau) \quad (5.3\text{-}7)$$

$$\ddot{\theta}_{c1} = e^{-3.68\tau}(4.14\times10^{2}\cos 42.2\tau - 3.60\times10^{1}\sin 42.2\tau) \quad (5.3\text{-}8)$$

$$\theta_{c6'} = e^{-3.68\tau}(7.16\times10^{-3}\sin 42.2\tau + 6.20\times10^{-4}\cos 42.2\tau)\times -1 \quad (5.3\text{-}9)$$

$$\dot{\theta}_{c6'} = e^{-3.68\tau}(3.02\times10^{-1}\sin 42.2\tau) \quad (5.3\text{-}10)$$

$$\ddot{\theta}_{c6'} = e^{-3.68\tau}(1.28\times10^{1}\cos 42.2\tau - 1.09\sin 42.2\tau) \quad (5.3\text{-}11)$$

These results (5.3-6) to (5.3-11) imply a time constant:

$$\Gamma_c = \frac{1}{\zeta W_n} = 0.2714 \text{ (sec)} \quad (5.3\text{-}12)$$

The amplitude of the engine angular velocity transient is:

$$|\dot{\theta}_{c1}| = 9.80 \times e^{-3.68\tau} \quad (5.3\text{-}13)$$

and the engine angular acceleration transient is:

$$|\ddot{\theta}_{c1}| = 416 \times e^{-3.68\tau} \quad (5.3\text{-}14)$$

(5.4) The Constant Response

For the step change imposed on the system equation (4.2-1) can be evaluated to give:

$$\alpha_{eng} = \frac{80-23.5}{4.702} = 12.0 \ (rad/sec^2) \qquad (5.4\text{-}1)$$

Equation (4.2-2) can be evaluated assuming α_{eng} is constant for the first second after the step change in T_{av} to produce:

$$\dot{\theta}_{ssc1} = 292 \ (rad/sec) \qquad (5.4\text{-}2)$$

The assumption of constant angular acceleration α_{eng} is not strictly true because T_{lc}' will increase due to the increase in speed (W_{eng}). This increase will reduce the magnitude of α_{eng} which thus does not remain constant.

(5.5) The Oscillatory Response

For the particular case under consideration the value $K_1 T_{av}$ is:

$$K_1 T_{av} = 200 \ (Nm) \qquad (5.5\text{-}1)$$

after the step input. Substitution of the physical constants of Table II into equations (4.3-1) and (4.3-2) will result in the following set of solutions:

$$\theta_{sso1} = 4.53 \times 10^{-3} \sin(560t - 0.869^{o}) \qquad (5.5\text{-}2)$$

$$\dot{\theta}_{sso1} = K_1 T_{av}(2W_e)(2.265 \times 10^{-5}) \cos(2W_e t - \Psi_1) \qquad (5.5\text{-}3)$$

$$= 2.54 \cos(560t - 0.869^{o})$$

$$\ddot{\theta}_{ss01} = -K_I T_{av}(4W_e^2)(2.265\times10^{-5})\sin(2W_e t - \Psi_1) \qquad (5.5\text{-}4)$$

$$= -1.43\times10^{3}\sin(560t - 0.869^{o})$$

$$\theta_{ss06}' = 6.02\times10^{-6}\sin(560t - 90^{o}) \qquad (5.5\text{-}5)$$

$$\dot{\theta}_{ss06}' = K_I T_{av}(2W_e)(3.01\times10^{-8})\cos(2W_e t - \Psi_6') \qquad (5.5\text{-}6)$$

$$= 3.37\times10^{-3}\cos(560t - 90^{o})$$

$$\ddot{\theta}_{ss06}' = K_I T_{av}(4W_e^2)(3.01\times10^{-8})\times -\sin(2W_e t - \Psi_6') \qquad (5.5\text{-}7)$$

$$= -1.88\sin(560t - 90^{o})$$

The solution (5.5-3) implies a final equilibrium engine angular velocity amplitude of:

$$|\ddot{\theta}_{ss01}| = 2.54 \quad (rad/sec) \qquad (5.5\text{-}8)$$

and a final equilibrium engine angular acceleration amplitude of:

$$|\ddot{\theta}_{ss01}| = 1420 \quad (rad/sec^2) \qquad (5.5\text{-}9)$$

The phase difference between the change in torque and the response is 0.0151 radians (0.869^{o}) or 5.39×10^{-5} sec at the original operating frequency (280 rad/sec).

6 COMPUTER SOLUTION OF THE NONLINEAR SYSTEM

The dynamics of the system of Figure 6 and equations (2.1-1) to (2.1-8) are simulated on the IBM 370 Computer using the CSMP language. The mean torque (T_{av}) and load torque (T_l) models given by equations (2.2.1-15) and (2.2.2.4-4) respectively are included in the simulation. The instantaneous torque (T_e) used in the simulation is computed using expression (2.2.1-2) rather than expression (2.2.1-3). The computer programs used are presented in Appendix IV.

The simulation is carried out for the same particular case as that given in Section (5.2) to facilitate comparison between the simulated and analytic results. Figure 12 illustrates the throttle input command step. Figure 13 illustrates the response of mean torque (T_{av}) to the throttle step input. Figure 14 and Figure 15 illustrate respectively the response of the engine rotational velocity and rotational acceleration to the throttle input.

The agreement between the analytic and simulated models is quite good as illustrated in Table III. No relative error between the two solutions exceeds 10%. What errors do occur can be explained. The calculations made in calculating both the transient response and the oscillatory response have

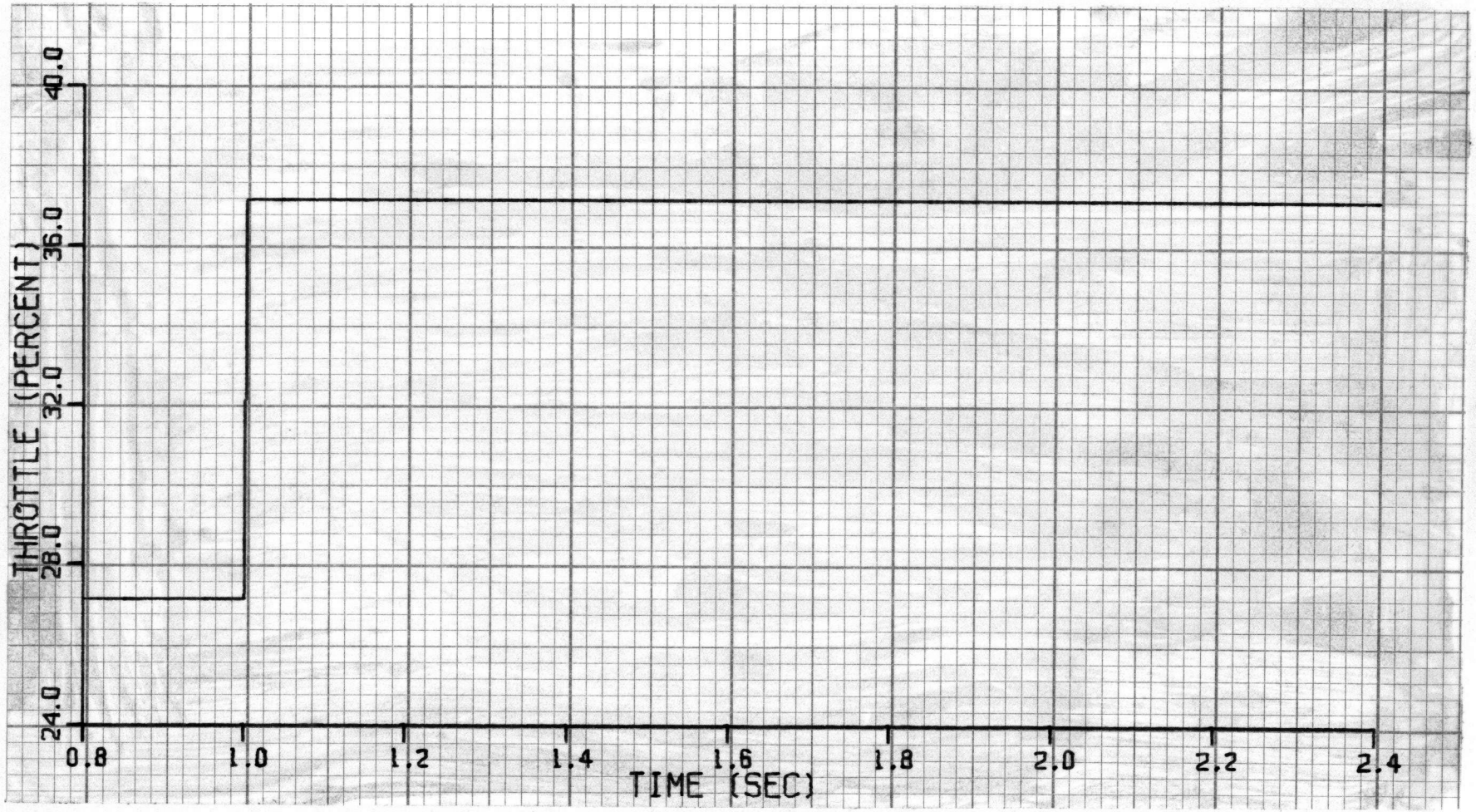

Figure 12: Throttle Command Input to the Computer Simulation Model

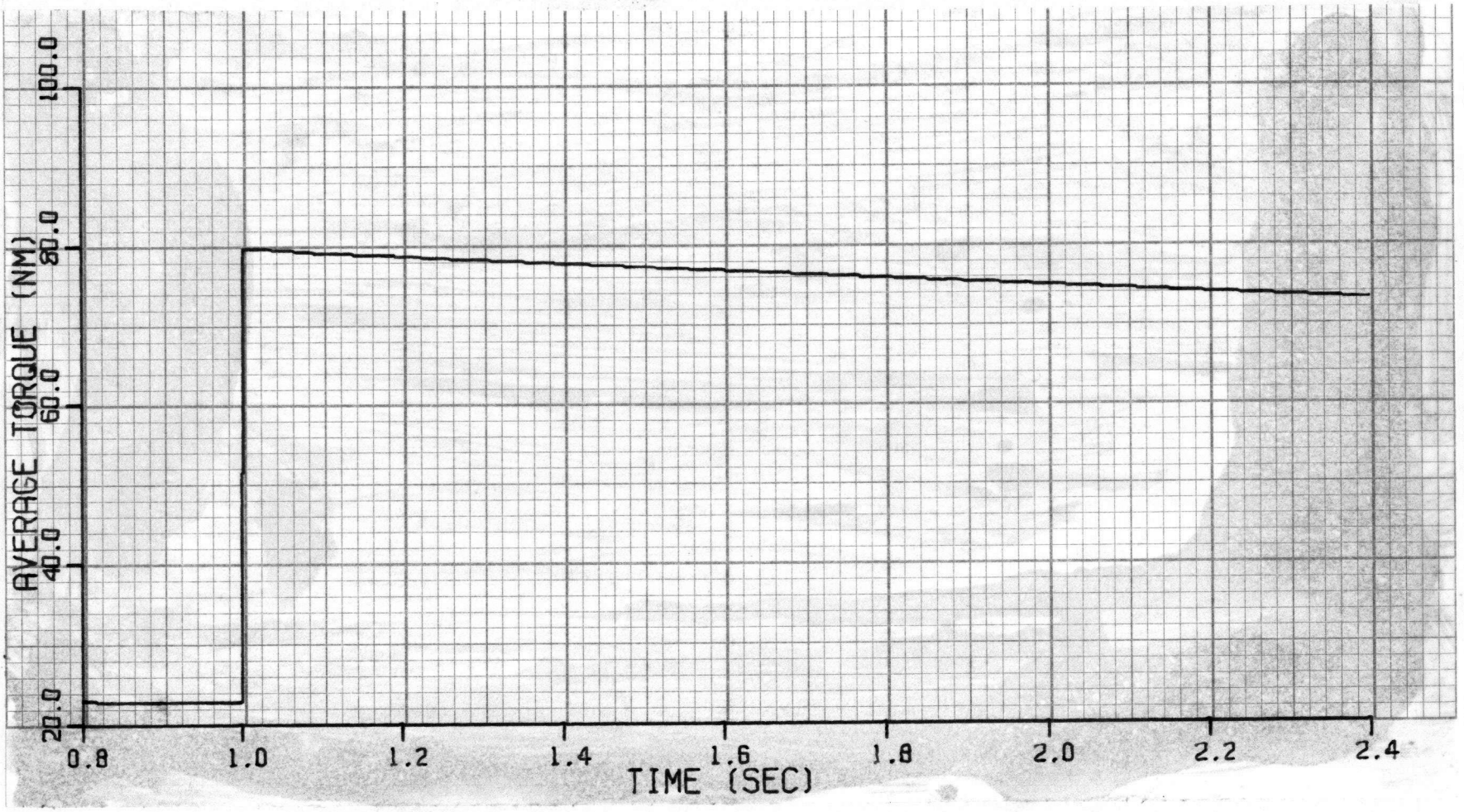

Figure 13: Mean Torque Response to the Throttle Command Input

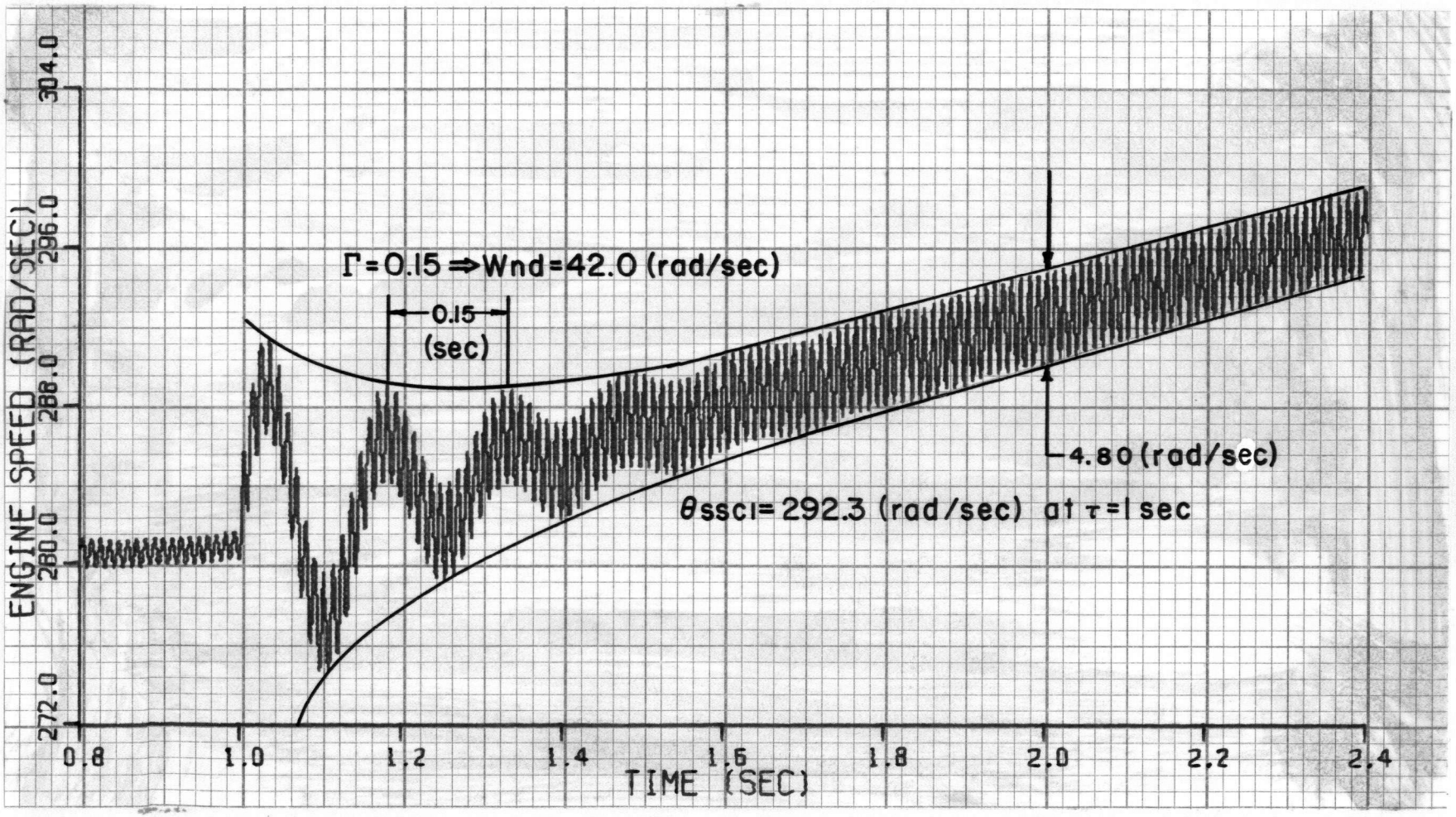

Figure 14: Engine Rotational Velocity Response to the Throttle Command Input

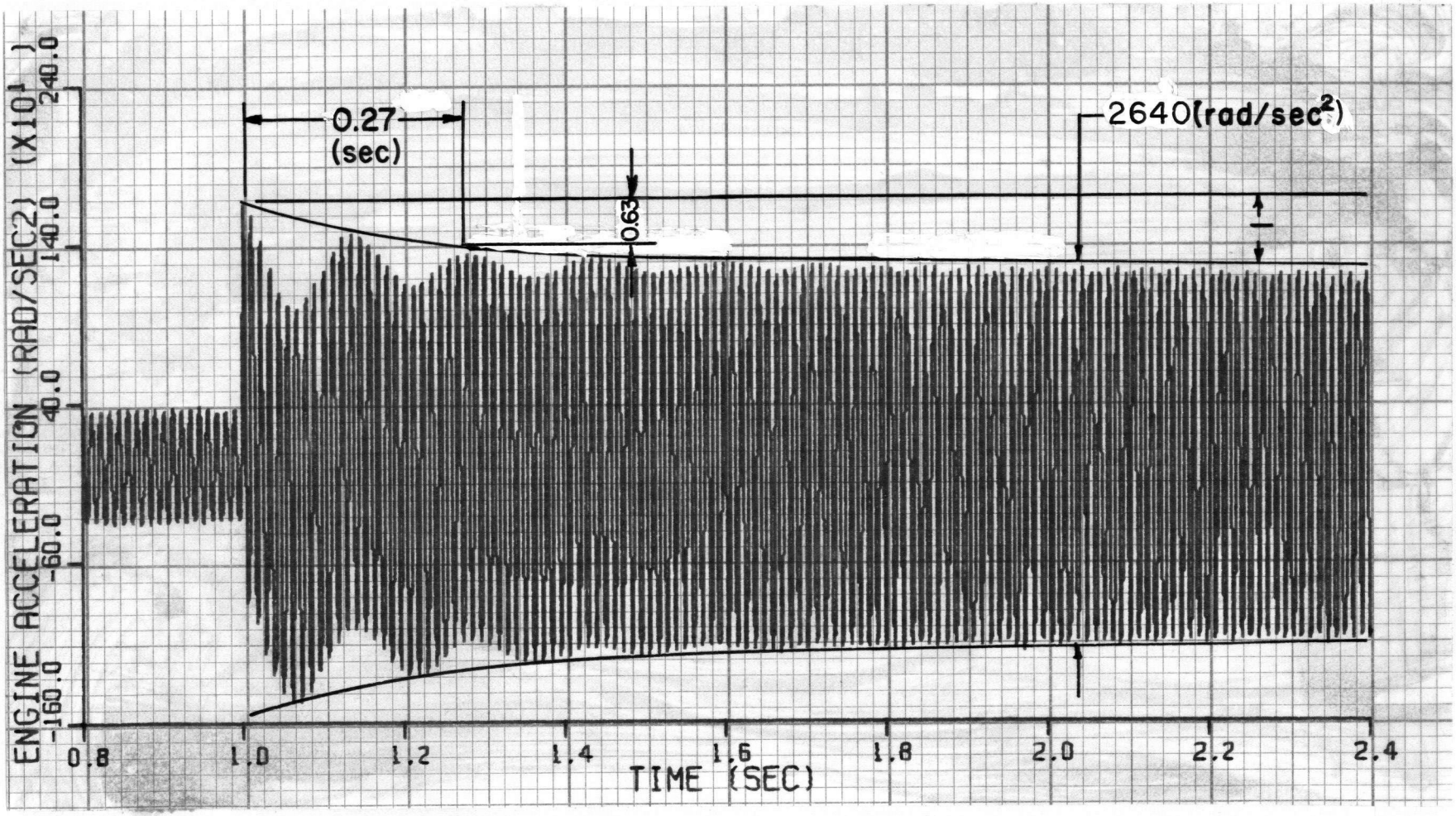

Figure 15: Engine Rotational Acceleration Response to the Throttle Command Input

TABLE III: COMPARISON OF ANALYTIC AND SIMULATED RESPONSES TO A STEP CHANGE IN ENGINE OUTPUT TORQUE (80-23.5-56.5 (Nm))

Item	Response		% Error Analytic/ Simulated
	Analytic	Simulated	
Transient Response (θ_{c1})			
Time Constant (Γ_c)	0.2714(sec)	0.27(sec)	0.5
Damped Natural Frequency (W_{nd})	42.2(rad/sec)	42.0(rad/sec)	0.5
Velocity Amplitude	9.80(rad/sec)	9.5(rad/sec)	3.0
Acceleration Amplitude	416(rad/sec)	400(rad/sec)	4.0
Forced Steady State Oscillatory Response (θ_{ss01})			
Velocity Amplitude	2.54(rad/sec)	2.40(rad/sec)	5.8
Acceleration Amplitude	1420(rad/sec^2)	1320(rad/sec^2)	7.6
Forced Steady State Constant Response (θ_{ssc1})			
Velocity at τ=1.0(sec) (Initial Velocity=280.0(rad/sec))	292(rad/sec)	292.3(rad/sec)	2.5

assumed that the frequency of the torque signal ($2\omega_e$) has remained constant. As Figure 14 shows this is clearly not the case. This assumption then can account for the error between these two solutions. For example, consider the oscillatory angular velocity amplitude as given by equation (5.5-8) this was calculated assuming ω_e=280 rad/sec but as shown in Figure 14 ω_e ranges from 280 to 294 rad/sec. This variation produces errors in the calculated response relative to the simulated response from 0 to 5%. Another error in the analytic results which has been pointed out previously is the assumption that α_{eng} is constant. This error explains the difference between the analytic and simulated constant velocity for τ=1 sec. The analytic model then, represents the dynamics of the simulated system closely.

The simulation model can be used to evaluate proposed control laws for adaptive controls. The law would be programmed and the response observed over a typical urban driving cycle. Air-fuel ratio control will require a further extension of the mean torque model given by equation (2.2.1-15).

7 MEAN TORQUE INDICATORS

Now that the analysis has been verified, the results can be used to investigate possible indicators of the mean torque. Inspection of the solutions (5.5-2) to (5.5-7) and (5.4-1) and (5.4-2) shows that they are all dependent on the mean torque (T_{av}). The transient solution (5.3-6) to (5.3-11) is also dependent on T_{av} for the special case of Section (5.2). A more detailed analysis of the potential observers follows.

(7.1) The Transient Response

The transient response will be excited by disturbances other than those in T_{av} thus making the boundary conditions and hence the response independent of T_{av}. Another problem posed by using the transient response as an indicator of torque is illustrated by Figure 16. The figure shows an initial transient followed by another transient beginning in the next cycle. Note that these transients have cancelled each other out. The cancellation means that no indication of the wrong indication of the change in torque may result from looking at the transient response.

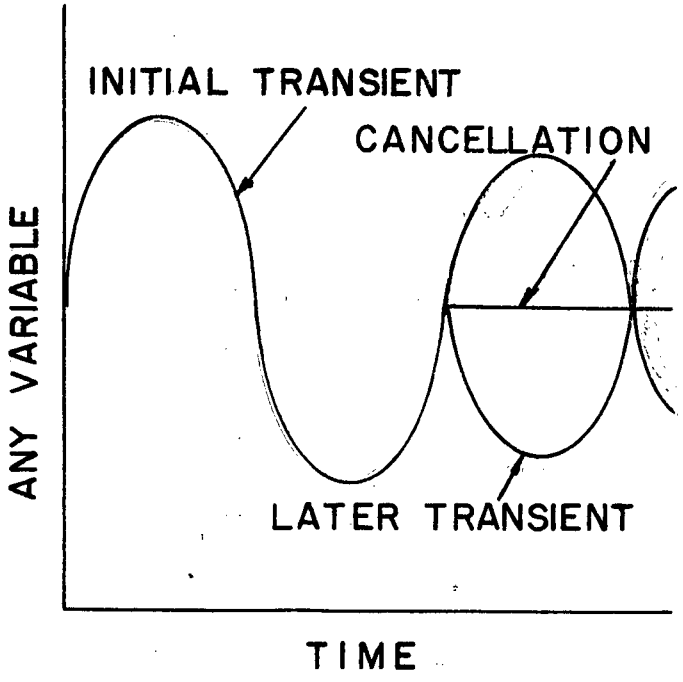

Figure 16: Transient Cancellation

(7.2) The Constant Response

The constant response could be used as an indicator of the mean torque. For example, measuring the gross vehicle acceleration or measuring the steady state constant part of the relative clutch angle will provide a signal of the constant response. The problem with using the gross vehicle acceleration is that it takes too long to see the effect due to a control change because of phase shift. With the control adjustment being on the order of every few cycles this lag will be unacceptable. Another serious problem arises because the constant response is also affected by disturbances in load. The constant response will not, therefore, always indicate how the engine mean torque is behaving because of the interference of these load torque disturbances.

(7.3) The Oscillatory Response

The steady state oscillatory response is dependent on the rotational frequency (We) as well as the mean torque (Tav). However, from one cycle to the next little change in speed will occur. As well, the speed changes tend to be in the same direction as the changes in mean torque, thus enhancing the indication of the change. The control would first observe the amplitude of the steady state oscillatory response, then adjust the spark timing and then observe the

steady state oscillatory amplitude of the first cycle after the adjustment. A comparison of the two amplitudes would then be made to determine the input to the controller of Figure 3.

The transient can be effectively separated from the steady state oscillatory response by a high pass filter. The transient frequency is always given by the damped natural frequency which in the case of the analysis carried out in this work is 42.6 rad/sec (400 rpm) and by design is kept well below the lowest operating frequency. The lowest frequency of the steady state oscillatory signal is twice the engine idle frequency or 160 rad/sec (1500 rpm). Therefore, there is normally a greater than fourfold separation of frequencies.

The steady state oscillatory acceleration has a much larger amplitude than the velocity signal as can be seen from inspection of equations (5.5-3) and (5.5-4). For this reason it will be a much easier signal to measure and changes in T_{av} will result in larger absolute changes in acceleration amplitude than in velocity amplitude.

The merits and drawbacks of all the responses as indicators of T_{av} are summarized in Table IV.

TABLE IV: EVALUATION OF SYSTEM RESPONSE SOLUTIONS AS INDICATORS OF MEAN TORQUE

Solution	Affected by Disturbances Other than in T_{av}	Frequency (rad/sec)	Amplitude	Phase (rad)
Transient				
θ_{c1}, $\dot{\theta}_{c1}$, $\ddot{\theta}_{c1}$	Yes	$W_{nd}=42.0$	depends on disturbances	depends on disturbance
Constant				
α_{eng}, ψ	Yes	-	depends on disturbance	-
Oscillatory				
θ_{ss01}	No	$2W_e$	$K_1 T_{av}(2.27\times10^{-5})$	0.0151
$\dot{\theta}_{ss01}$			$2W_e K_1 T_{av}(2.27\times10^{-5})$	
$\ddot{\theta}_{ss01}$			$4W_e^2 K_1 T_{av}(2.27\times10^{-5})$	

8 CONCLUSIONS

A simplified linear model of the dynamics of the internal combustion engine vehicle driver system has been developed. This model is verified by comparison with a computer simulation model which includes the important nonlinearities. The linear model is shown to be a good approximation of its simulated counterpart. Models describing the engine mean torque, are also developed.

The problems of measuring the mean torque are discussed. It is established that measuring one of the engine variables will provide the best observer for the mean torque. Other variables downstream of the engine are subject to phase shifts and attenuation. The solutions obtained for these variables from the linear model have been used in the evaluation and selection of the best engine variable. It is shown that the transient and constant solutions are excited by disturbances in the load torque as well as by disturbances in the engine mean torque. This fact rules them out as potential observers of the mean torque.

The evaluation and selection has determined that the steady state oscillatory acceleration response provides the best indication of the mean torque. A system has b

9 RECOMMENDATIONS FOR FUTURE WORK

Future work should be directed towards the development of a device for measuring the oscillatory acceleration. As well, the structure and quantitative determination of the adaptive controller should be pursued. To achieve the latter goal the simulation model developed in this work should be extended to include the human, adaptive and feedback models. The simulation model would then be a useful tool in the design, selection and optimization of adaptive control for internal combustion engines.

REFERENCES

[1] Myers, P.S., Uyehara, O.A., Newhall, H.K., "The ABC's of Engine Exhaust Emissions", Engineering Know How in Engine Design - Part 19, Society of Automotive Engineers, SP-365, 1971.

[2] Anonymous, "Air Pollution: The Problem and the Risks", SAE Journal, Volume 76, No. 3, May, 1968, pp. 47-52.

[3] Anonymous, "Fuel Economy and Emission Controls", United States Environmental Protection Agency Office of Air and Water Programs Mobile Source Pollution Control Program, November, 1972.

[4] Conta, L.D., "The Control of Automotive Emissions", American Society of Mechanical Engineers, No. 73-WA/DGP-3, November, 1973.

[5] Stempel, R.C., and Martins, S.W.., "Fuel Economy Trends and Catalytic Converters", Society of Automotive Engineers, No. 740594, August, 1974.

[6] LaPoint, C., "Factors Affecting Fuel Economy", Automotive Engineering, Volume 81, No. 11, November, 1973, pp. 46-50.

[7] Anonymous, "Present and Future Trends in Auto Fuel Consumption", Automotive Engineering, Volume 81, No. 7, July, 1973, pp. 48-50.

[8] Schweitzer, Paul H., "Control of Exhaust Pollution Through a Mixture Optimizer", Society of Automotive Engineers, No. 72025, January, 1972.

[9] Schweitzer, Paul H., Volz, Carl, and Deluca, Frank, "Control System to Optimize Engine Power", Society of Automotive Engineers, No. 700884, November, 1970.

[10] Kehres, John K., and Allan, John J., "Exhaust Pollution Minimization in Small Engines Using Adaptive Digital Control", Society of Automotive Engineers, No. 730858, 1973.

[11] Adams, T.N., "Adaptive Control and Performance Indicators for Internal Combustion Engines", Private Communication, 1973.

[12] Williams, M., "A Digital Memory Fuel Controller for Gasoline Engines", Society of Automotive Engineers, No. 720282, January, 1972.

[13] Soltav, J.P., Senior, K.B., and Rowe, B.B., "Digitally Programmed Engine Fuelling Controls", Society of Automotive Engineers, No. 730128, January, 1973.

[14] Rivard, J.G., "Closed Loop Electronic Fuel Injection Control of the Internal-Combustion Engine", Society of Automotive Engineers, No. 730005, January, 1973.

[15] Hubbard, M., and Powell, J.D., "Closed Loop Control of Internal Combustion Engine Exhaust Emissions", Guidance and Control Laboratory, Department of Aeronautics and Astronautics, Stanford University, SUDAAR No. 473, February, 1974.

[16] Westcott, J.H., An Exposition of Adaptive Control, London, England, Pergamon Press, 1961.

[17] Kronauer, R.E., and Drew, P.G., "Design of Adaptive Feedback Loop in Parameter Perturbation Adaptive Controls", Theory of Self-Adaptive Control Systems, Proceedings of the Second IFAC Symposium on the Theory of Self-Adaptive Control Systems, Plenum Press, New York, 1966, pp. 299-308.

[18] Taylor, C.V., The Internal Combustion Engine in Theory and Practice, Volume II: Combustion, Fuels, Materials, Design, Cambridge, Massachusetts, M.I.T. Press, 1968.

[19] Yamamoto, Kenichi, Rotary Engine, Toyo Kogyo Lo. Ltd., October, 1971.

[20] Hoerner, S.F., Fluid Dynamic Drag, Sighard F. Hoerner, Midland Park, N.J., pp. 12-1 to 12-8.

[21] Den Hartog, J.P., Mechanical Vibrations, McGraw Hill Book Company, New York, N.Y., 1956, pp. 374-375.

[22] Shigley, J.E., Dynamic Analysis of Machines, McGraw Hill Book Company, New York, N.Y., 1956

[23] Davisson, J.A., "Design and Application of Commercial Type Tires", Society of Automotive Engineers, No. 690001, January, 1969.

[24] Cortina Shop Manual, Service Publications, Ford of Britain, May, 1972.

[25] Baumeister, T., Editor in Chief, Standard Handbook for Mechanical Engineers, Seventh Edition, McGraw Hill Book Company, 1966.

APPENDIX I: EQUATIONS OF MOTION OF AN INTERNAL COMBUSTION ENGINE VEHICLE SYSTEM

(AI.1) Purpose

The purpose of this Appendix is to derive the equations of motion (2.2-1) to (2.2-8) which apply to Figure 6. The important assumptions made in making the lumped parameter system approximation are presented and their validity investigated.

(AI.2) Assumptions

The assumptions made in the lumped parameter model are; all inertias other than the engine and load inertias are neglected, all springs in the system other than the tires, driveshaft or clutch are assumed rigid and damping effects other than those of the clutch and tires are ignored.

(AI.2.1) Inertia Assumptions

The components having the largest inertias next to the engine are the gears, clutch plates and driveshaft. The inertia of a typical gear (I_g), a typical clutch plate (I_{cp}) and a typical driveshaft (I_{ds}) are presented below:

$$I_g = \frac{1}{2} m_g \cdot r_g^2 \qquad \text{(AI.2.1-1)}$$

where: m_g = mass of gear = $\rho(\pi \cdot r_g^2)t$ = 1.54 ($Nsec^2/m$)

ρ = density of steel = 7.89×10^{-3} ($Nsec^2/(m)cm^3$)

r_g = gear radius = 5.0 (cm)

t = gear thickness = 2.5 (cm)

$$\therefore I_g = 0.00194 \ (Nmsec^2/rad) \qquad \text{(AI.2.1-2)}$$

$$I_{cp} = \frac{1}{2} m_c \cdot r_c^2 \qquad \text{(AI.2.1-3)}$$

where: m_c = mass of clutch = 0.72 ($Nsec^2/m$)

r_c = clutch radius = 10.79 (cm)

$$\therefore I_{cp} = 0.00419 \ (Nmsec^2/rad) \qquad \text{(AI.2.1-4)}$$

$$I_{ds} = \frac{1}{2} m_{ds}(r_o^2 - r_i^2) \qquad \text{(AI.2.1-5)}$$

where: m_{ds} = mass of driveshaft = 4.4 ($Nsec^2/m$)

r_o = outside diameter of driveshaft = 2.5 (cm)

r_i = inside diameter of driveshaft = 2.35 (cm)

$$\therefore I_{ds} = 0.00016 \ (Nmsec^2/rad) \qquad \text{(AI.2.1-6)}$$

These inertias are all at least two orders of magnitude smaller than the engine inertia of 0.14 ($Nmsec^2/rad$). Therefore, the inertias of these components as well as smaller components may be safely neglected.

(AI.2.2) Spring Assumptions

The components having the lowest spring rates will generally be those of smallest cross sectional area, greatest length or made of the most flexible material (e.g. tires). The torsional spring constant of shafts in the system is inversely proportional to their lengths. Therefore, shafts such as the crankshaft, will be essentially rigid when compared with the driveshaft. The spring constant for a section of crankshaft is given by:

$$Kcs = \frac{\pi g G dcs^2}{32 l} \qquad \text{(AI.2.2-1)}$$

where: G=shear modulus of steel=8.45×10^5 ($Nsec^2/(m)cm^2$)

g=acceleration of gravity=9.8 (m/sec^2)

dcs=5.699 (cm)

l=2.54 (cm)

$$\therefore Kcs = 5.96 \times 10^5 \text{ (Nm/rad)} \qquad \text{(AI.2.2-2)}$$

This spring constant is two orders of magnitude greater than the driveshaft spring constant of:

$$Ks = 7800 \text{ (Nm/rad)} \qquad \text{(AI.2.2-3)}$$

The assumption that all components of the system other than the tire, driveshaft or clutch are rigid is thus established.

(AI.2.3) Damping Assumptions

Equation (5.3-2) illustrates that the damping ratio ζ is in the range 0.1. Other forms of damping present in the system include structural damping (ζ=0.01), journal bearing

friction (ζ=0.001) and gear friction (ζ=0.001). The effects of these damping mechanisms are ignored because their contribution to the motion of the system is very small when compared with that of the clutch and tire.

(AI.2.4) Limitations of Analysis

Several factors have not been considered in this analysis which may be of importance in later work. Among these factors is the engagement and disengagement analysis of the clutch, the effect of the differential upon the vehicle dynamics and the analysis of slipping of the rear wheels.

(AI.3) Equations of Motion

Figure 6 may be used to draw free body diagrams of the system components to obtain the equations of motion.

(AI.3.1) The Engine

Figure 17 is a free body diagram of the engine idealized as a pure inertia J_e. A torque T_e is imposed on this system and torque T_1 results. The analysis of this system produces the following result:

$$T_e - J_e \ddot{\theta}_e = T_1 \qquad \text{(AI.3.1-1)}$$

(AI.3.2) The Clutch

Figure 18 is a free body diagram of the clutch idealized as a parallel spring (K_c) and nonlinear coulomb damper (T_c).

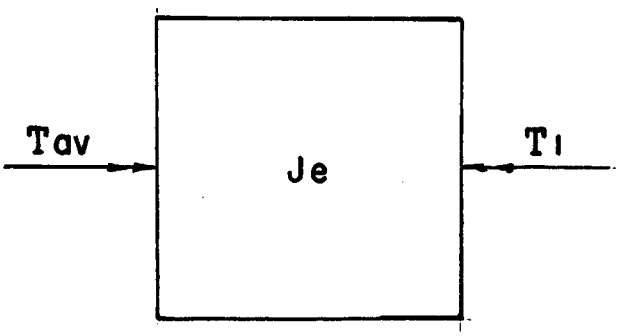

Figure 17: Free Body Diagram of Engine

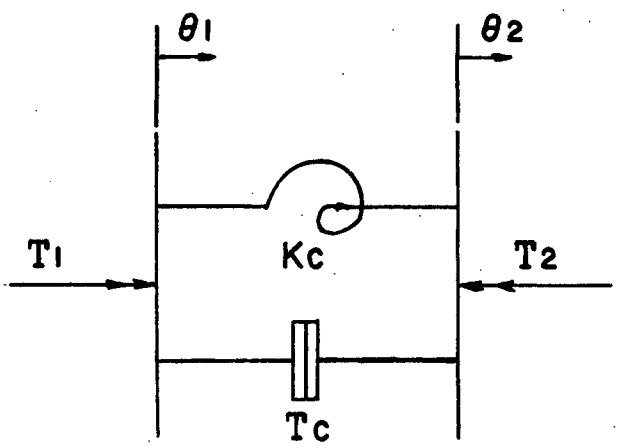

Figure 18: Free Body Diagram of Clutch

The torque in T_1 is equal to the torque out T_2 and is given by:

$$T_1 = K_c(\theta_1 - \theta_2) + T_c \qquad \text{(AI.3.2-1)}$$

where T_c is the value of the nonlinear coulomb damping.

(AI.3.3) The Transmission

The free body diagram of Figure 19 illustrates the transmission. The following equations result from this system:

$$\theta_2 = \theta_3 \times R_g \qquad \text{(AI.3.3-1)}$$

$$R_g \times T_2 = T_3 \qquad \text{(AI.3.3-2)}$$

where R_g is the gear ratio.

(AI.3.4) The Driveshaft

Figure 20 presents the free body diagram of the driveshaft which is idealized as a spring (K_s). The equations of motion of this system are:

$$T_3 = T_4 \qquad \text{(AI.3.4-1)}$$

$$T_3 = K_s(\theta_3 - \theta_4) \qquad \text{(AI.3.4-2)}$$

(AI.3.5) The Rear End

Figure 21 which is much the same as Figure 19 is the free body diagram of the rear end which is an ideal transformer. The analysis produces the following results:

$$T_5 = R \times T_4 \qquad \text{(AI.3.5-1)}$$

$$\theta_4 = R \times \theta_5 \qquad \text{(AI.3.5-2)}$$

(AI.3.6) The Tires

Figure 22 is the free body diagram of the tires. The tires are idealized as a parallel combination of a spring (K_t).

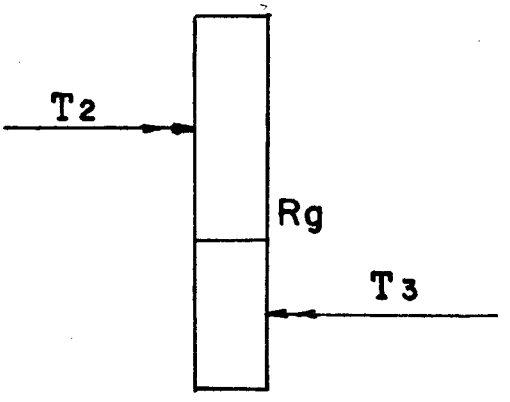

Figure 19: Free Body Diagram of Transmission

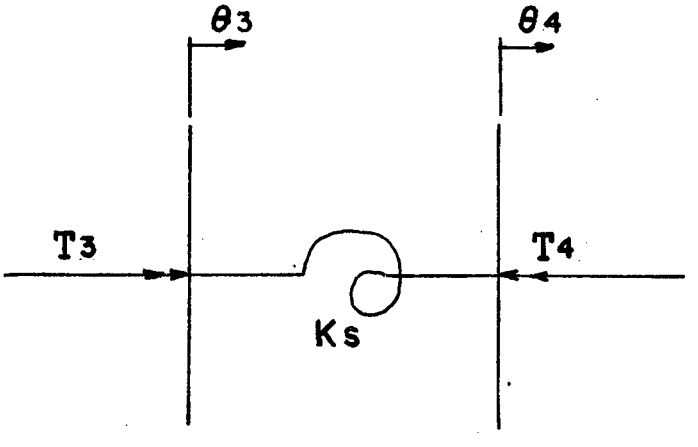

Figure 20: Free Body Diagram of Driveshaft

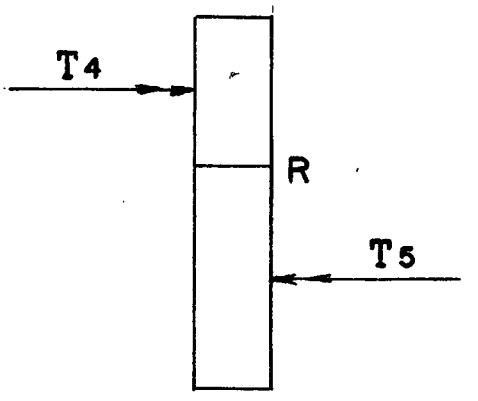

Figure 21: Free Body Diagram of Rear End

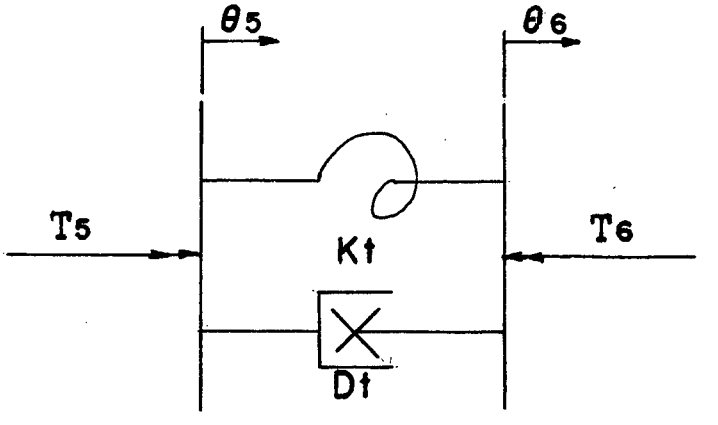

Figure 22: Free Body Diagram of Tires

and a damper (D_t). Analysis of the system shows:

$$T_5 = T_6 \qquad \text{(AI.3.6-1)}$$

$$T_5 = K_t(\theta_5 - \theta_6) + D_t(\dot{\theta}_5 - \dot{\theta}_6) \qquad \text{(AI.3.6-2)}$$

(AI.3.7) The Load

Figure 23 is the free body diagram of the load idealized as a pure inertia (J_l). The inputs to the system are the torque T_6 and T_l. T_l is the load torque which is a function of speed. The investigation of this system provides the following equation of motion:

$$T_l + J_l\ddot{\theta}_6 = T_6 \qquad \text{(AI.3.7-1)}$$

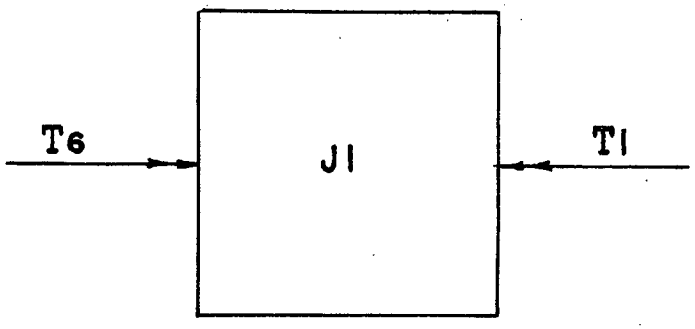

Figure 23: Free Body Diagram of Load

APPENDIX II: SOLUTIONS OF THE EQUATIONS OF MOTION OF THE LINEAR EQUIVALENT SYSTEM

(AII.1) Homogeneous Solution

The homogeneous equations of motion are:

$$Je\ddot{\theta}_{c1} + Deq(\dot{\theta}_{c1} - \dot{\theta}_{c6'}) + Keq(\theta_{c1} - \theta_{c6'}) = 0 \qquad \text{(AII.1-1)}$$

$$Jl'\ddot{\theta}_{c6'} + Deq(\dot{\theta}_{c6'} - \dot{\theta}_{c1}) + Keq(\theta_{c6'} - \theta_{c1}) = 0 \qquad \text{(AII.1-2)}$$

The solutions of these equations are of the form:

$$\theta_{c1} = \theta_{a1} \times e^{s\tau} \qquad \text{(AII.1-3)}$$

$$\theta_{c6'} = \theta_{a6'} \times e^{s\tau} \qquad \text{(AII.1-4)}$$

where $s = -p + iq$ and p is the negative of the exponent of decay of the amplitude while q is the damped natural frequency. Substituting (AII.1-3) and (AII.1-4) into (AII.1-1) and (AII.1-2) results in:

$$\left[Je\,s^2\theta_{a1} + Deq\,s(\theta_{a1} - \theta_{a6'}) + Keq(\theta_{a1} - \theta_{a6'})\right]e^{s\tau} = 0 \qquad \text{(AII.1-5)}$$

$$\left[Jl's^2\theta_{a6'} + Deqs(\theta_{a6'} - \theta_{a1}) + Keq(\theta_{a6'} - \theta_{a1})\right]e^{s\tau} = 0 \qquad \text{(AII.1-6)}$$

Rewriting (AII.1-5) and (ALL.1-6) produces the following results:

$$\frac{\theta_{a1}}{\theta_{a6'}} = \frac{Deqs + Keq}{Je\,s^2 + Deqs + Keq} \qquad \text{(AII.1-7)}$$

$$\frac{\theta_{a6'}}{\theta_{a1}} = \frac{Jl's^2 + Deqs + Keq}{Deqs + Keq} \qquad \text{(AII.1-8)}$$

Equating (AII.1-7) and (AII.1-8) results in the frequency equation:

$$\frac{JeJl'}{Je+Jl'}s^2+Deqs+Keq=0 \qquad \text{(AII.1-9)}$$

Equation (AII.1-9) can be solved to produce the following result:

$$s=\frac{-Deq\pm\sqrt{Deq^2-4\left(\frac{JeJl'}{Je+Jl'}\right)Keq}}{2\left(\frac{JeJl'}{Je+Jl'}\right)} \qquad \text{(AII.1-10)}$$

This result can be evaluated knowing the numerical values of Je, Jl', Deq and Keq The final solution can be written in the form:

$$\theta c1=e^{-p\tau}(A\cos q\tau+B\sin q\tau) \qquad \text{(AII.1-11)}$$

$$\theta c6'=De^{-p\tau}(A\cos q\tau+B\sin q\tau) \qquad \text{(AII.1-12)}$$

$$p=\frac{Deq}{2Jeq} \quad \text{(the real part of AII.1-10)} \qquad \text{(AII.1-13)}$$

$$q=\sqrt{\frac{Keq}{Jeq}-\frac{Deq^2}{4Jeq^2}} \quad \text{(the imaginary part of AII.1-10)} \qquad \text{(AII.1-14)}$$

The value of D can be calculated from either equation (AII.1-7) or (AII.1-8) and is:

$$D=\frac{\theta a6'}{\theta a1} \qquad \text{(AII.1-15)}$$

A and B are arbitrary constants which are evaluated from the system boundary conditions.

(AII.2) Constant Solution

The steady state constant equations of motion are:

$$Je\ddot{\theta}ssc1 + Deq(\dot{\theta}ssc1 - \dot{\theta}ssc6') + Keq(\theta ssc1 - \theta ssc6') = Tav \quad \text{(AII.2-1)}$$

$$Jl'\ddot{\theta}ssc6' + Deq(\dot{\theta}ssc6' - \dot{\theta}ssc1) + Keq(\theta ssc6' - \theta ssc1) = Tlc' \quad \text{(AII.2-2)}$$

where Tlc' is the constant part of the equivalent load torque.

Now the solution of these equations are:

$$\ddot{\theta}ssc1 = \ddot{\theta}ssc6' = \alpha eng \quad \text{(AII.2-3)}$$

$$\dot{\theta}ssc1 = \dot{\theta}ssc6' = Wengi + \int \alpha eng\, d\tau \quad \text{(AII.2-4)}$$

$$\theta ssc1 - \theta ssc6' = \psi \quad \text{(AII.2-5)}$$

where αeng is the engine angular acceleration, $Wengi$ is the initial engine angular velocity and ψ is the angular deflection.

Substituting the results (AII.2-3) to (AII.2-5) into (AII.2-1) and (AII.2-2) produces;

$$\alpha eng = \frac{Tav - Tlc'}{Je + Jl'} \quad \text{(AII.2-6)}$$

and

$$\psi = \frac{Tav}{Keq} - \frac{Je(Tav - Tlc')}{Keq(Je + Jl')} \quad \text{(AII.2-7)}$$

In the special case where $\alpha eng = 0$ the result (AII.2-7) reduces to:

$$\psi = \frac{Tav}{Keq} \quad \text{(AII.2-8)}$$

(AII.3) Oscillatory Solution

The steady state forced oscillatory equations of motion are:

$$Je\,\ddot{\theta}_{ss01} + Deq(\dot{\theta}_{ss01} - \dot{\theta}_{ss06'}) + Keq(\theta_{ss01} - \theta_{ss06'}) = T_{avo} \quad \text{(AII.3-1)}$$

$$Jl'\ddot{\theta}_{ss06'} + Deq(\dot{\theta}_{ss06'} - \dot{\theta}_{ss01}) + Keq(\theta_{ss06'} - \theta_{ss01}) = -T_{lo'} \quad \text{(AII.3-2)}$$

In these equations $T_{lo'}$ represents the fluctuating part of the load torque and T_{avo} represents the fluctuating part of the engine torque. These two factors are given by:

$$T_{lo'} = C_2\,\dot{\theta}_{ss06'} \quad \text{(AII.3-3)}$$

and

$$T_{avo} = K_1 T_{av} \sin 2We\,t \quad \text{(AII.3-4)}$$

Assuming the solutions of equations (AII.3-11) and (AII.3-2) are of the form:

$$\theta_{ss01} = |\theta_{ss01}|\,e^{+i2Wet} \quad \text{(AII.3-5)}$$

$$\theta_{ss06'} = |\theta_{ss06'}|\,e^{+i2Wet} \quad \text{(AII.3-6)}$$

the following equations result:

$$\left[-Je\,4We^2|\theta_{ss01}| + Deq\,2iWe(|\theta_{ss01}| - |\theta_{ss06'}|) + Keq(|\theta_{ss01}| - |\theta_{ss06'}|)\right] e^{i2Wet} = K_1 T_{av}\, e^{i2Wet} \quad \text{(AII.3-7)}$$

$$\left[-Jl'4We^2|\theta_{ss06'}| + Deq\,2iWe(|\theta_{ss06'}| - |\theta_{ss01}|) + Keq(|\theta_{ss06'}| - |\theta_{ss01}|)\right] e^{i2Wet} = -C_2\,2iWe|\theta_{ss06'}|\,e^{i2Wet} \quad \text{(AII.3-8)}$$

These equations can be rewritten to produce:

$$\left[Keq + Deq\,2Wei - Je4We^2\right]|\theta_{ss01}| - \left[Deq\,2Wei + Keq\right]|\theta_{ss06'}| = K_1 T_{av} \quad \text{(AII.3-9)}$$

$$\left[Keq+(Deq+C_2)2Wei-JI'(4We^2)\right]|\theta sso6'|-\left[Deq\,2Wei+Keq\right]|\theta sso1|=0 \qquad \text{(AII.3-10)}$$

These equations can be solved by using Cramer's Rule:

$$|\theta sso1|=\frac{\begin{vmatrix} KITav & (Deq\,2Wei+Keq) \\ 0 & (Keq+(Deq+C_2)2Wei-JI'4We^2) \end{vmatrix}}{\begin{vmatrix} (Keq+Deq\,2Wei-Je\,4We^2)\,(Deq\,2Wei+Keq) \\ (Deq\,2Wei+Keq)(Keq+(Deq+C_2)2Wei+JI'4We^2) \end{vmatrix}} \qquad \text{(AII.3-11)}$$

$$|\theta sso6'|=\frac{\begin{vmatrix} (Keq+Deq\,2Wei-Je\,4We^2) & KITav \\ (Deq\,2Wei+Keq) & 0 \end{vmatrix}}{\begin{vmatrix} (Keq+Deq2Wei-Je\,4We^2)\,(Deq\,2Wei+Keq) \\ (Deq\,2Wei+Keq)(Keq+(Deq+C_2)2Wei+JI'4We^2) \end{vmatrix}} \qquad \text{(AII.3-12)}$$

Once the values of the physical constants and the operating frequency are known, equations (AII.3-11) and (AII.3-12) can be evaluated. The final results will be of the form:

$$\theta sso1=A1\sin(2Wet+\psi 1) \qquad \text{(AII.3-13)}$$

$$\theta sso6'=A6'\sin(2Wet+\psi 6') \qquad \text{(AII.3-14)}$$

where $A1, A6', \psi 1$ and $\psi 6'$ are evaluated using equations (AII.3-11) and (AII.3-12).

APPENDIX III: PHYSICAL CONSTANTS USED IN THE ANALYSIS

(AIII.1) Purpose

The purpose of this Appendix is to present the sources and derivation of the physical constants used in the analysis in Sections 2,3,4, and 5.

(AIII.2) Engine Inertia (Je)

Figure 24 illustrates the flywheel and crankshaft layout in the Cortina 2000 c.c. engine. Figure 25 illustrates a connecting rod, piston pin and piston from the same engine. Both Figures 24 and 25 are somewhat idealized and were constructed from data taken from [24].

(AIII.2.1) Weight of Piston

The weight of the piston is determined by evaluating the following:

$$Wp = \frac{\rho g}{4}\left[\pi(do^2 - di^2)h1 + \pi do^2 h2\right] \qquad \text{(AIII.2.1-1)}$$

where the symbols are as shown in Figures 24 and 25, except that:

ρ = density of steel = 7.89×10^{-3} $(Nsec^2/(m)cm^3)$

g = acceleration of gravity = 9.8 (m/sec^2)

$$\therefore Wp = 9.75 \text{ (N)} \qquad \text{(AIII.2.1-2)}$$

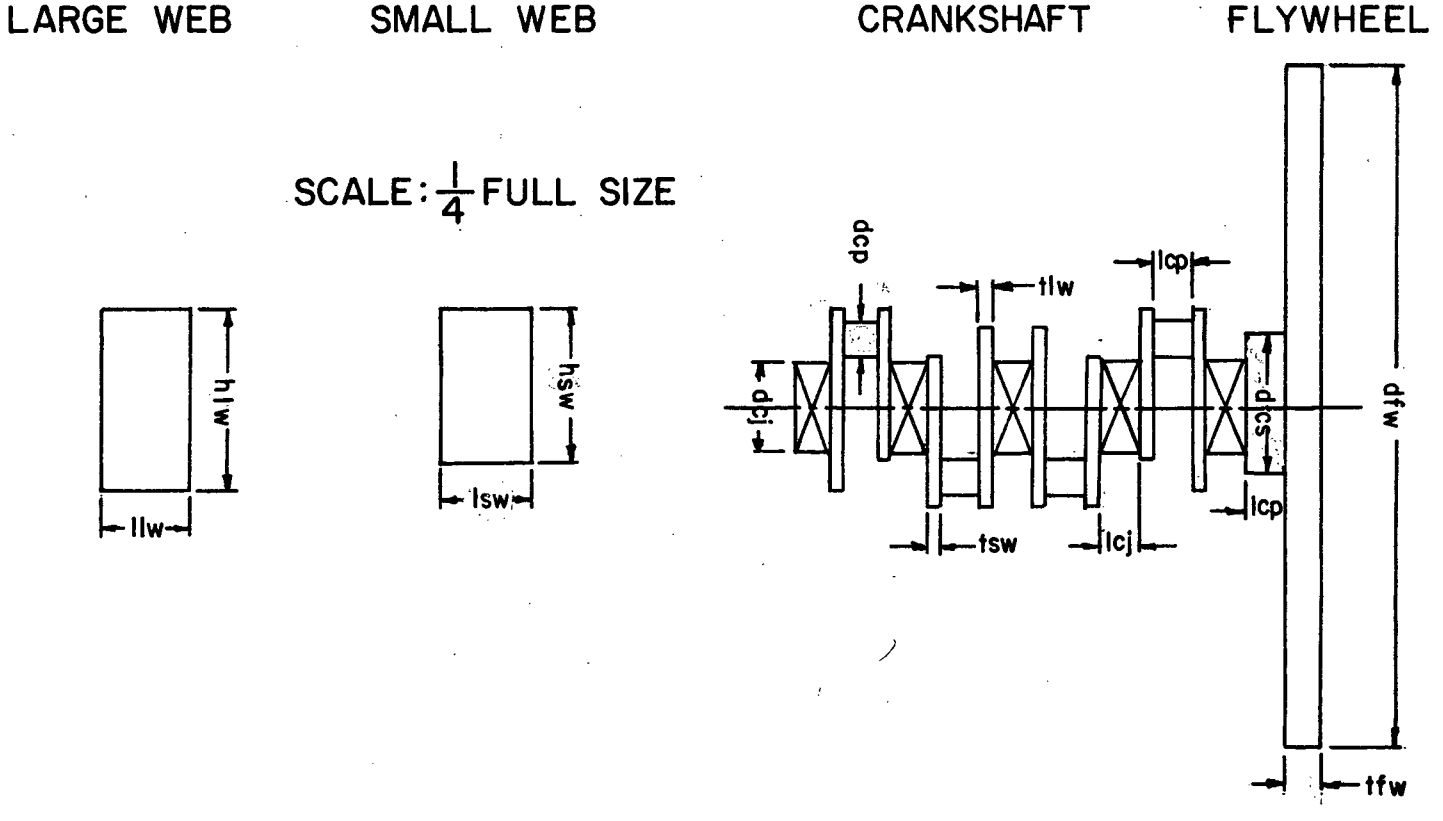

Figure 24: Flywheel and Crankshaft Layout of Cortina 2000 c.c. Engine

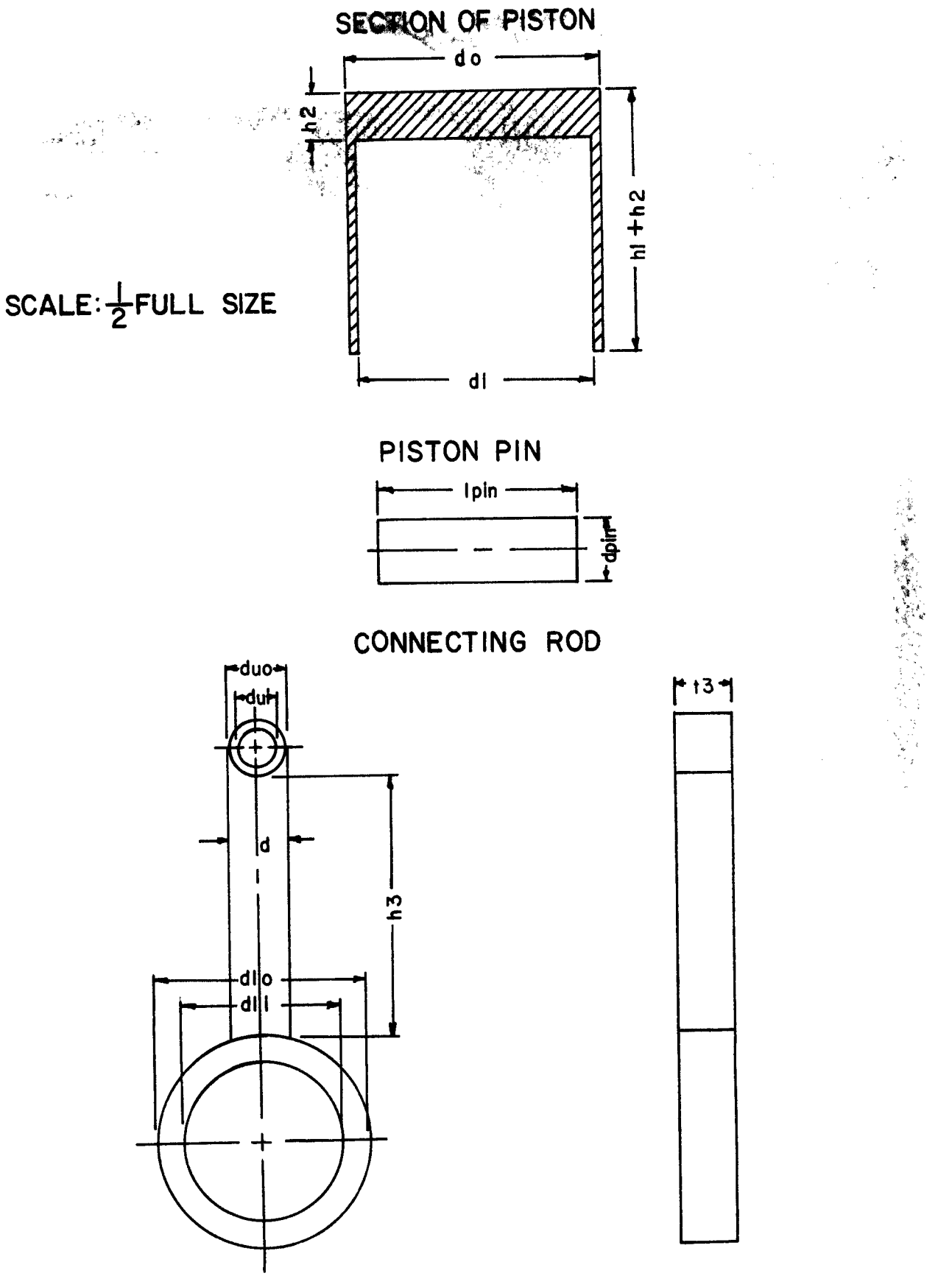

Figure 25: Connecting Rod, Piston Pin and Piston of Cortina 2000 c.c. Engine

(AIII.2.2) Weight of Piston Pin

The weight of the piston pin is given from:

$$W_{pin} = \frac{\rho g \cdot \pi \cdot l_{pin} \cdot d_{pin}^2}{4} = 2.519 \quad (N) \qquad \text{(AIII.2.2-1)}$$

(AIII.2.3) Weight of the Connecting Rod

The weight of the connecting rod is given by:

$$W_{cr} = \rho g t_3 \left[\frac{\pi(d_{uo}^2 - d_{ui}^2)}{4} + h_{3d} + \frac{\pi(d_{lo}^2 - d_{li}^2)}{4} \right] \qquad \text{(AIII.2.3-1)}$$

$$\therefore W_{cr} = 5.297 \quad (N)$$

(AIII.2.4) Weight of Crank Journal

The weight of the crank journal is calculated from:

$$W_{cj} = \frac{\rho g}{4} \pi \cdot d_{cj}^2 \cdot t_{cj} = 5.01 \quad (N) \qquad \text{(AIII.2.4-1)}$$

(AIII.2.5) Weight of Crank Pin

The weight of the crank pin is given by:

$$W_{cp} = \frac{\rho g}{4} \pi \cdot d_{cp}^2 \cdot t_{cp} = 4.171 \quad (N) \qquad \text{(AIII.2.5-1)}$$

(AIII.2.6) Weight of Small Web)

The weight of the small web is given by:

$$W_{sw} = \rho g \cdot l_{sw} \cdot h_{sw} \cdot d_{sw} = 4.175 \quad (N) \qquad \text{(AIII.2.6-1)}$$

(AIII.2.7) Weight of Large Web

The weight of the large web is given by:

$$Wlw = llw \cdot dlw \cdot hlw \cdot \rho g = 6.089 \quad (N) \qquad \text{(AIII.2.7-1)}$$

(AIII.2.8) Weight and Inertia of Reciprocating Mass

Dividing the connecting rod mass so that one third is reciprocating and two thirds is rotating the total reciprocating weight becomes:

$$Wrm = Wp + Wpin + \frac{1}{3} Wcr = 14.03 \quad (N) \qquad \text{(AIII.2.8-1)}$$

The moment of inertia of the reciprocating masses is:

$$Irm = \frac{Wrm}{g}(Stroke \times 0.5) = 2.12 \times 10^{-3} \ (Nmsec^2) \qquad \text{(AIII.2.8-2)}$$

(AIII.2.9) Inertia of Rotating Portion of the Connecting Rod

The moment of inertia of the rotating mass of the connecting rod is:

$$Ircr = \frac{Wcr(Stroke)^2}{6g} = 5.33 \times 10^{-4} \quad (Nmsec^2) \qquad \text{(AIII.2.9-1)}$$

(AIII.2.10) Inertia of Crank Journal

The moment of inertia of the crank journal is:

$$Icj = \frac{Wcj rcj^2}{2g} = 2.08 \times 10^{-4} \quad (Nmsec^2) \qquad \text{(AIII.2.10-1)}$$

(AIII.2.11) Inertia of Crank Pin

The moment of inertia of the crank pin with respect to its own centre of mass is:

$$Icp(cm) = \frac{Wcp \cdot rcp^2}{2g} = 1.438 \times 10^{-4} \quad (Nmsec^2) \qquad \text{(AIII.2.11-1)}$$

Using the parallel axis theorem this inertia is transferred to the crank journal axis:

$$I_{cp/cj} = I_{cp(cm)} + \frac{W_{cp}\, r_{cp/cj}^2}{2g} = 6.3\times10^{-4}\ (Nmsec^2) \qquad \text{(AIII.2.11-2)}$$

(AIII.2.12) Inertia of Large Web

The moment of inertia of the large web relative to its centre of mass is:

$$I_{lw(cm)} = \frac{W}{12g}\,(l_w^2 + h_{lw}^2) = 8.246\times10^{-4}\ (Nmsec^2) \qquad \text{(AIII.2.12-1)}$$

The moment of inertia of the large web transferred to the crank journal axis is:

$$I_{lw/cj} = 9.14\times10^{-4} \quad (Nmsec^2) \qquad \text{(AIII.2.12-2)}$$

(AIII.2.13) Inertia of Small Web

The moment of inertia of the small web is calculated in a similar manner as that of the large web. Its value is:

$$I_{sw/cj} = 4.36\times10^{-4} \quad (Nmsec^2) \qquad \text{(AIII.2.13-1)}$$

(AIII.2.14) Total Inertia Associated With One Cylinder

The total inertia associated with one cylinder is found from:

$$I_{cyl} = I_{rm} + I_{rcr} + I_{cj} + I_{cp/cj} + I_{lw/cj} + I_{sw/cj} = 4.84\times10^{-3}\ (Nmsec^2)$$

(AIII.2.14-1)

(AIII.2.15) Weight and Inertia of Flywheel

The weight of the flywheel is given as:

$$Wfw = \frac{\rho g \cdot \pi dfw^2 \cdot tfw}{4} = 120.9 \quad (N) \qquad \text{(AIII.2.15-1)}$$

where: dfw=28.0 (cm) (flywheel diameter)

tfw=2.54 (cm) (flywheel thickness)

The moment of inertia of the flywheel is:

$$Ifw = \frac{Wfw \cdot rfw^2}{2g} = 1.21 \times 10^{-1} \quad (Nmsec^2) \qquad \text{(AIII.2.15-2)}$$

(AIII.2.16) Weight and Inertia of Shaft Between Crank and Flywheel

The weight of the connecting shaft is:

$$Ws = \rho g \cdot \pi \cdot rs^2 \cdot ls = 8.769 \quad (N) \qquad \text{(AIII.2.16-1)}$$

The moment of inertia of this shaft is given by:

$$Is = \frac{Ws \cdot rs^2}{2g} = 6.46 \times 10^{-4} \quad (Nmsec^2) \qquad \text{(AIII.2.16-2)}$$

(AIII.2.17) The Total Inertia of The Engine

The total inertia of the engine is given by:

$$Je = 4Icyl + Is + Ifw = 0.141 \quad (Nmsec^2/rad) \qquad \text{(AIII.2.17-1)}$$

(AIII.3) Clutch Spring (Kc) and Damper (Tc) Constants

The clutch spring and damping constants were determined from experiments with a small (16.5cm in diameter) clutch. The results are then extrapolated to the Cortina clutch (21.5cm in diameter).

Figure 26 illustrates the experimental setup. Figure 27 presents the results of the experiment. The intercept of the straight line is the static damping torque which is:

$$Tcs = 6.0 \quad (Nm) \tag{AIII.3-1}$$

The dynamic damping torque can be calculated knowing the ratio of the dynamic friction coefficient to the static friction coefficient for the clutch plate material. This ratio is found to be 0.53 for asbestos [25]. The dynamic damping torque is then:

$$Tcd = 3.2 \quad (Nm) \tag{AIII.3-2}$$

The slope of the straight line given in Figure 27 gives the spring constant. Thus the spring constant is given by:

$$Kc = 1030 \quad (Nm/rad) \tag{AIII.3-3}$$

As a check, the spring constant is calculated. Figure 28 illustrates the dimensions and arrangement of the clutch plate used in the experiment. The spring constant of one spring of the clutch plate is:

$$Kci = \frac{G\,d^4}{8nD^3} = 2.32 \times 10^5 \quad (N/m) \tag{AIII.3-4}$$

where: G=shear modulus of steel=7.92×10^{10} (N/m^2)

A one Newton force acting on this spring is equivalent to a torque of:

$$1\ \text{Newton} \times \frac{dcs}{2} = 3.5 \times 10^{-2}\ (Nm) \tag{AIII.3-5}$$

Therefore, the spring constant Kci may be written:

$$Kci = 284.0 \quad (Nm/rad) \tag{AIII.3-6}$$

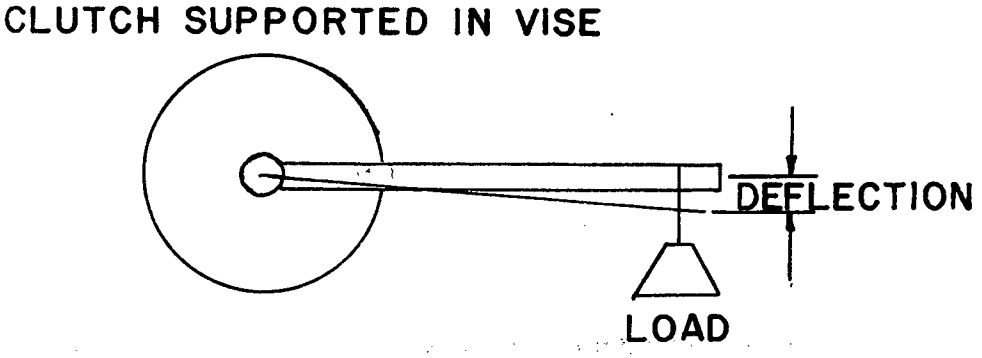

Figure 26: Experimental Setup for Determining Clutch Spring and Damping Constants

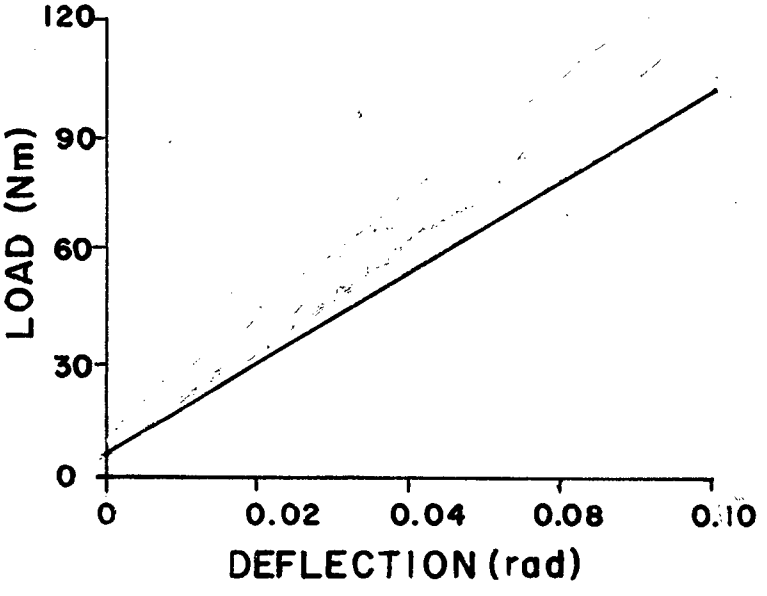

Figure 27: Results of the Clutch Experiment

Figure 27: Experimental Setup for Determin
Clutch Spring and Damping C

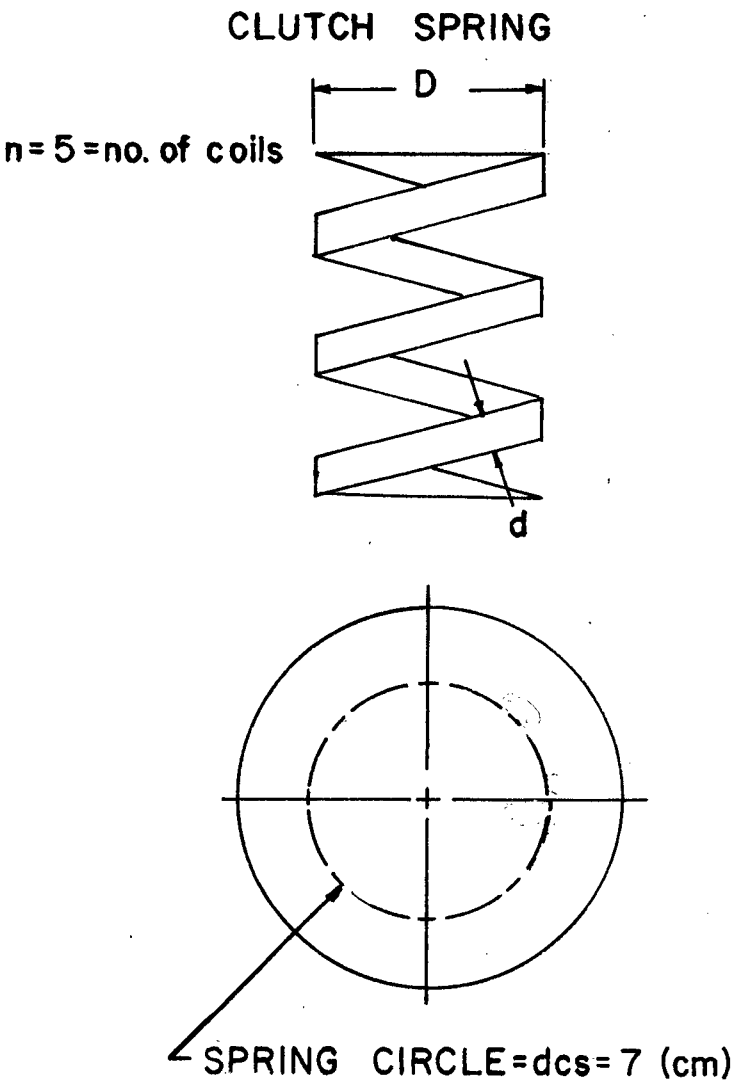

Figure 28: Clutch Plate and Springs

The total spring constant is the sum of the individual spring constants or:

$$Kc = 4 \times Kci = 1140 \quad (Nm/rad) \qquad \text{(AIII.3-7)}$$

Comparison of the results indicates that the disagreement is less than 10%.

Scaling the spring constants linearly with clutch diameter produces the following result:

$$Kc = 1500 \quad (Nm/rad) \qquad \text{(AIII.3-8)}$$

The damping torque is not affected by any change in size.

(AIII.4) Gear Ratios (Rg)

The gear ratios are found in [24]. They are:

Gear	Ratio
1st	3.65
2nd	1.97
3rd	1.37
4th	1.00

(AIII.4-1)

(AIII.5) Driveshaft Spring Constant (Ks)

The driveshaft spring constant is calculated using the dimensions illustrated in Figure 29. The resulting value is:

$$Ks = \frac{G\pi(do^4 - di^4)}{321} = 7800 \quad (Nm/rad) \qquad \text{(AIII.5-1)}$$

(AIII.6) Rear End Ratio (R)

The rear end ratio is given in [24] as:

$$R = 3.44 \qquad \text{(AIII.6-1)}$$

l=length=244 (cm)
di=4.8 (cm)
do=5.0 (cm)

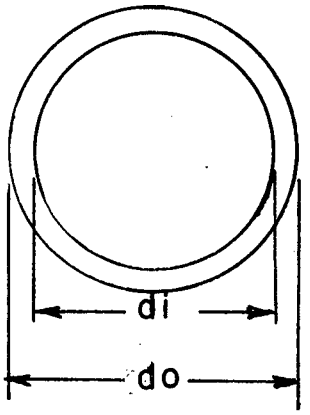

Figure 29: Driveshaft Dimensions

(AIII.7) Tire Spring (Kt) and Damping (Dt) Constants

The tire spring and damping constants are reported in [23]. The average spring constant is:

$$Kt=6950 \quad (Nm/rad) \tag{AIII.7-1}$$

and the average damping constant is:

$$Dt=58.0 \quad (Nmsec/rad) \tag{AIII.7-2}$$

(AIII.8) Load Inertia (Jl)

Figure 30 is a free body diagram of the vehicle and one of its wheels. The force F acting on the wheels can be written:

$$F=\mu Nr \tag{AIII.8-1}$$

where Nr is the portion of the vehicle weight over the rear wheels. The vehicle weight is given in [24] as 11,100 (N). The weight distribution is 45% rear and 55% front. The coefficients of friction between the tire and a dry road is found in [25] to be μ=0.8. Therefore:

$$F=4995 \quad (N) \tag{AIII.8-2}$$

The maximum acceleration achieved by the vehicle is calculated from:

$$amax=\frac{F}{m}=4.41 \quad (m/sec) \tag{AIII.8-3}$$

At the rear wheels, the maximum torque developed is given by:

$$Tmax=Rw\times F \tag{AIII.8-4}$$

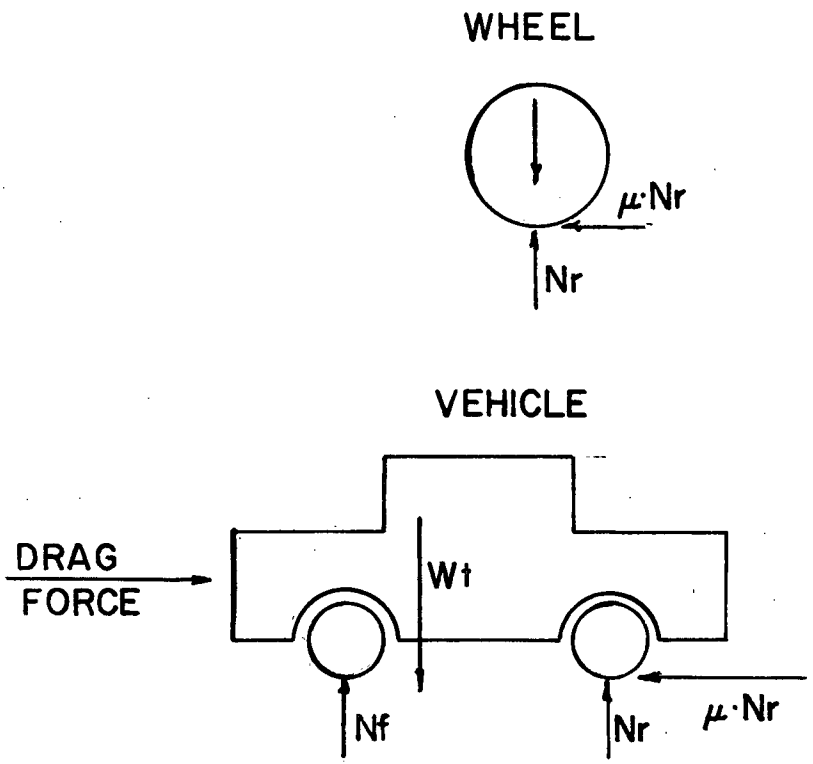

Figure 30: Free Body Diagram of Vehicle

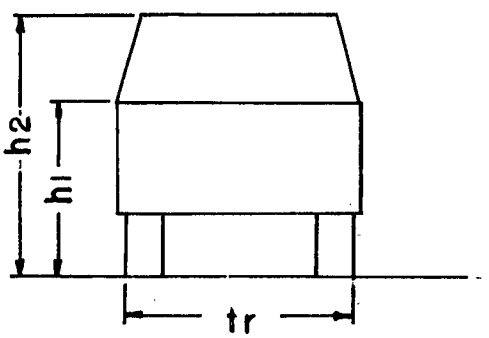

Figure 31: Front View of Cortina Sedan

where **Rw** is the dynamic wheel radius given in [25] as:

$$Rw = 0.2997 \quad (m) \qquad \text{(AIII.8-5)}$$

for the Cortina tires. The maximum torque is related to the vehicle inertia by:

$$T_{max} = J_I \alpha_{max} \qquad \text{(AIII.8-6)}$$

where $\alpha_{max} = \frac{a_{max}}{r} = 14.71 \ (rad/sec^2)$

Therefore, the vehicle inertia is given as:

$$J_I = \frac{T_{max}}{\alpha_{max}} = 102 \quad (Nm\,sec^2/rad) \qquad \text{(AIII.8-7)}$$

(AIII.9) Vehicle Frontal Area (Ap)

Figure 31 is a front view of the Cortina sedan. The frontal area is calculated with the aid of this Figure and is given by:

$$A_p = (h_1 - h_2) \times t_r = 1.53 \quad (m^2) \qquad \text{(AIII.9-1)}$$

AIII.10 Engine Torque Coefficients

The engine torque coefficients used in equation (2.2.1-2) are given in References [18] as:

C2=1.2	B2=-0.1
C4=0.2	B4=-0.02
C6=0.05	B6=-0.008
C8=0.01	B8=-0.005

APPENDIX IV: COMPUTER PROGRAM

The purpose of this Appendix is to present the computer program used in the simulation of Section 6.

The program is stored in the file ICFILE (a listing of this file appears in this Appendix) under the ID CNTL. The statements in the INITIAL and TERMINAL sections may require revision from run to run. To execute the program the following sequence of commands is required:

```
$SIG CNTL
Password
$R *CSMPTRAN SCARDS=ICFILE
$R *FORTRAN SCARDS=-CSMP#7
$R *CSMPEXEC-LOAD#+*CSMPLIB 5=-CSMP#5 SPRINT=DFILE
```

This sequence will place the results of the simulation in the file DFILE.

```
1       MACRO ZZ=NONLIN(AACC,I,J,CANVEL,RELTOR)
2       PROCEDURAL
3             XX=DELAY(I,J,RELTOR)
4             YY=ABS(XX)
5             WW=DELAY(I,J,CANVEL)
6             VV=ABS(WW)
7             IF(TIME-P1.LE.0.0) GO TO 107
8             IF(VV-0.1) 100,100,101
9       100   ZZ=XX
10            IF(YY-6.0) 102,102,103
11      103   IF(ZZ.GT.6.0) GO TO 104
12            ZZ=-3.2
13            GO TO 102
14      107   ZZ=AACC
15            GO TO 102
16      104   ZZ=3.2
17            GO TO 102
18      101   IF(WW.GT.3.0) GO TO 105
19            ZZ=-3.2
20            GO TO 102

21       105   ZZ=3.2
22       102   CONTINUE
23       ENDMAC
24       *THE ABOVE MACRO DESCRIPTION MODELS THE NONLINEAR CLUTCH DYNAMICS
25       MACRO SS=DLAY(AABB,N,PA,ANVEL)
26       PROCEDURAL
27             W=DELAY(N,PA,ANVEL)
28             V=W
29             IF(TIME-PA.LE.0.0) GO TO 108
30             SS=V*R*RG
31             GO TO 109
32       108   SS=AABB
```

```
      109   CONTINUE
      ENDMAC
      MACRO TT=ANGLE(NN,ANGE,PK,N)
      PROCEDURAL
            QQ=DELAY(N,PK,ANGE)
      111   PP=QQ-NN*2.0*3.1416
            IF(PP-2.0*3.1416.LE.0.0) GO TO 110
            NN=NN+1
            GO TO 111
      110   TT=2.0*PP
      ENDMAC
      *THE ABOVE MACRO DESCRIPTION CALCULATES THE CRANKSHAFT ANGULAR
      *DISPLACEMENT
      INITIAL
      *THIS SECTION DEFINES THE SYSTEM PARAMETERS AND INITIAL CONDITIONS
            MEMORY NONLIN
            MEMORY DLAY
            MEMORY ANGLE
      PARAMETER JE=0.14,JL=102.0,KC=1500.0,KT=6950.0,KS=7800.0,DT=58.0,...
      R=3.44,RG=1.37,P1=0.0005,P2=0.001,P3=0.0015,P4=0.002,P5=0.0025,...
      P6=0.003,P7=0.0035,P8=0.004,P9=0.0045,P10=0.005,P11=0.0055,P12=0.006,...
      P13=0.0065,P14=0.007,P15=0.0075,P16=0.008,P17=0.0085,P18=0.009,...
      P19=0.0095,P20=0.01,P21=0.0105,P22=0.011,P23=0.0115,P24=0.012,...
      P25=0.0125,P26=0.013,P27=0.0135,P28=0.014,P29=0.0145,P30=0.015,N2=1,...
      C2=1.2,C4=0.2,C6=0.05,C8=0.01,B2=-0.1,B4=-0.02,B6=-0.008,B8=-0.005
      INCON IC1=280.0,IC2=0.126,IC3=0.0132,IC5=0.0,IC6=0.0
            IC4=IC1/(R*RG)
      DYNAMIC
      *THIS SECTION MODELS THE DYNAMICS OF THE SYSTEM
            FREQ=DLAY(IC1,1,P1,SITLC)
            TMAX=93.4+0.355*THRCT
      *THROTTLE INPUT
            THROT=27.1+10.0*STEP(1.0)
```

```
66          SOTHEO=3.86*THROT
67      *AVERAGE TORQUE
68          TAV=TMAX*(1.0-0.275*(((FREQ/SOTHEO)-1.0)**2))
69          SOTOR=ANGLE(N2,SOTHE,P1,1)
70      *INSTANTANEOUS ENGINE TORQUE
71          SOTE=TAV*(1.0+C2*2*SIN(SOTOR)+C4*4*SIN(2*SOTOR)+...
72          B2*2*COS(SOTOR)+B4*4*COS(2*SOTOR)+C6*6*SIN(3*SOTOR)+...
73          C8*8*SIN(4*SOTOR)+B6*6*COS(3*SOTOR)+B8*8*COS(4*SOTOR))
74      *LOAD TORQUE
75          SOTR=37.5+(0.0152*(S1TLO**2))+SOTRD
76      *LOAD TORQUE DISTURBANCES
77          SOTRD=0.0
78      *SYSTEM EQUATIONS OF MOTION
79          S2THE=SOTE/JE+SOTHE2*KC/JE-SOTD/JE-KC*SOTHE/JE
80          S1THE=INTGRL(IC1,S2THE)
81          SOTHE=INTGRL(IC2,S1THE)
82          SOTHE2=(SOTD*(RG**2)+KC*(RG**2)*SOTHE+KS*RG*SOTHE4)/...
83          (KC*(RG**2)+KS)
84          SOTHE3=SOTHE2/RG
85          SOT4=KS*(SOTHE3-SOTHE4)
86          SOTHE4=R*SOTHE5
87          S1THE5=R*SOT4/DT+KT*SOTLO/DT+S1TLO-KT*SOTHE5/DT
88          SOTHE5=INTGRL(IC3,S1THE5)
89          S2TLO=(DT*S1THE5+KT*SOTHE5-SOTR-DT*S1TLO-KT*SOTLO)/JL
90          S1TLO=INTGRL(IC4,S2TLO)
91          SOTLO=INTGRL(IC5,S1TLO)
92          S1THE2=DERIV(IC1,SOTHE2)
93          S1CLUT=S1THE-S1THE2
94          SOCLUT=SOTHE-SOTHE2
95          SOTD=NONLIN(IC6,1,P1,S1CLUT,SORR)
96          SORR=SOTE-SOTR/(R*RG)-JL*S2TLO/(R*RG)-JE*S2THE
97          SOJE=JE*S2THE
98          SOCS=KC*(SOCLUT)
```

```
 99      NOSORT
100      *OUTPUT PRINTER CONTROL
101            TIMEI=TIMEI+DELT
102            IF(TIMEI-2.0*DELT.EQ.0.0) GO TO 117
103            GO TO 118
104      117   TIMEI=0.0
105            WRITE(6,116) TIME,TAV,THROT,S1THE,S2THE
106      116   FORMAT(5E12.4)
107      118   CONTINUE
108      SORT
109      TERMINAL
110      *THIS SECTION CONTROLS THE EXECUTION PHASE OF THE MODEL
111      TIMER FINTIM=3.0,PRDEL=0.01,DELT=0.0005
112      METHOD RECT
113      END
114      STOP
115      ENDJOB
116      $END
```